



*DEMETRA - 3D prEcision farMing using intErnet of Things
and unmanned aeRiAl vehicles in greenhouses*

**DELIVERABLE D3.1
TECHNOLOGY CONCEPT AND TECHNICAL REQUIREMENTS,
SCENARIOS AND KPIs
MAY 31, 2023**

**STELIOS IOANNOU, MARIOS RASPOPOULOS, ANDREY SESYUK AND
DEMETRIS KALLASIDES**
INTERDISCIPLINARY SCIENCE PROMOTION & INNOVATIVE RESEARCH EXPLORATION (INSPIRE)



**Co-funded by
the European Union**



**RESEARCH
& INNOVATION
FOUNDATION**

"This work was co-funded by the European Union under the programme of social cohesion "THALIA 2021-2027", through Research and Innovation Foundation (Project: CONCEPT/0722/0100)".

Abstract

This report describes the concept, requirements and specifications of the technologies investigated in the project as well as the use case scenarios and the respective KPIs for the validation and verification of the system components and prototypes.

Table of Contents

List of Figures	5
List of Tables.....	7
1 Introduction to the Project.....	8
1.1 Concept and Objectives.....	8
1.2 Innovation and Originality	8
1.3 Added Value and Benefits	9
1.3.1 References.....	9
1.4 Aims and Objectives	10
1.4.1 Aim	10
1.4.2 Technical Objectives.....	10
1.4.3 Operational Requirements	11
2 Literature Review	12
2.1 Precision Agriculture Applications	12
2.1.1 References.....	13
2.2 Smart Green Houses.....	16
2.2.1 References.....	22
2.3 Image Processing Algorithms for Small Unmanned System Applications.....	26
2.3.1 References.....	27
2.4 3D Positioning and Tracking Using AI Cameras	31
2.4.1 References:.....	32
2.5 Indoor 3D Positioning Using mmWave Technology.....	35
2.5.1 References.....	36
2.6 Insects Present in Cyprus.....	38
2.6.1 References.....	41

2.7	Commercially Available Cameras for Image Processing Applications	42
2.7.1	References.....	44
2.8	Commercially Available Spectral Cameras for Small Unmanned System Applications	45
2.8.1	References.....	49
2.9	Commercially Available UAV for DEMETRA Project.....	51
2.9.1	References.....	52
2.10	Commercially Available Sensors for Greenhouse Applications.....	53
2.10.1	Controller: STM32 Nucleo-F303RE Microcontroller	53
2.10.2	Display: uLCD-144-G2	54
2.10.3	Temperature & Humidity sensor - DHT-11	54
2.10.4	pH Sensor - SEN0161-V2.....	55
2.10.5	Air Quality Sensor - MQ-135.....	56
2.10.6	Light Intensity Sensor – Custom made Using GL5516 LDR	57
2.10.7	Soil Moisture Sensor – Custom made.....	58
2.10.8	References.....	58
2.11	Vegetation Indexes.....	61
2.11.1	NDVI (Normalized Difference Vegetation Index)	63
2.11.2	(NDWI) Normalized Difference Water Index	65
2.11.3	OSAVI (Optimized Soil-Adjusted Vegetation Index)	67
2.11.4	NDRE (Normalized Difference Red Edge Index)	67
2.11.5	GNDVI (Green Normalized Difference Vegetation Index)	68
2.11.6	LCI (Leaf chlorophyll index).....	68
2.11.7	References.....	68
2.12	Commercially Available mmWave Radar Sensors.....	70
3	Used Cases and Scenarios	72
3.1.1	Indoor Cluttered Environment	72
3.1.2	Indoor Open space Environment.....	73

3.1.3	Outdoor Open Space Environment	74
4	Metrics/Key Performance Indicators and Targets	75
4.1	Precision Analysis KPIs.....	75
4.2	3D Positioning Analysis KPIs	75
5	Technical Specifications.....	77
5.1	Hardware.....	77
5.2	Software	77
6	Summary of all Proposed KPIs	78
6.1	Greenhouse Mentoring System.....	78
6.2	Image Processing.....	78
6.3	UAV Flight and Multispectral Data Collection.....	79
6.4	Multispectral Image Processing.....	79
6.5	Indoor Positioning	79
6.6	Indoor Positioning by GPS Conversion and Retransmission	79

List of Figures

Figure 1: PA Block Diagram Derived from Literature	13
Figure 2: Gothic Type Green House	17
Figure 3: Dr. Panos's Smart-Greenhouse (Panos, 2021)	17
Figure 4: Folium Wireless Multisensors (FarmRoad®, 2022)	18
Figure 5: Planty Greenhouse in Larnaca, Cyprus (Planty, 2020)	20
Figure 6: Nutrition film technique (NFT) (Planty, 2020)	20
Figure 7 Spodoptera littoralis(SPODLI)	39
Figure 8 Spodoptera littoralis (adult).....	39
Figure 9 Early 3rd instar.....	39
Figure 10 Fully grown larva	39
Figure 11 Egg cluster on chrysanthemum.	39
Figure 12 4th instar.	39
Figure 13 Atherigona orientalis adult, dorsal view	40
Figure 14 cucumber mosaic virus	40
Figure 15 Atherigona orientalis late stage damage of pepper fruits	40
Figure 16 Cucumber mosaic virus on chilli pepper	40
Figure 17 Comstockaspis perniciosa.....	40
Figure 18 Comstockaspis perniciosa infestation on apple branch.....	40
Figure 19 Liriomyza huidobrensis	40
Figure 20 Leaf mines on Liriomyza huidobrensis.....	40
Figure 21 Symptoms of Pepino mosaic virus on cherry tomatoes.....	41
Figure 22 Leaf blistering symptoms from Pepino mosaic virus(PEPMV0)	41
Figure 23: AVIOTEC IP Starlight 8000 Video-Based Fire Detection. (Bosch, 2016)	42
Figure 24: Fixed-Mount Thermal Camera FLIR A50/A70 Smart Sensor. (FLIR, 2022)	42
Figure 25: SR7FIRE-MD-DUAL system (thermal visible camera) for fire detection on industrial environment	42
Figure 26: OAK SoM for depth and AI processing.....	43
Figure 27: Hyperspectral vs. Multispectral data [1].....	45
Figure 28: Visible and IR light spectrum [2]	45
Figure 29: Wavelength and Band Allocation [3]	46
Figure 30: Hyperspectral Narrower Bands [3]	46
Figure 31: Hyperspectral camera with DJI M300 Drone [4]	48
Figure 32: Nano HP (400-1000nm) Hyperspectral Imaging Package [5].....	48

Figure 33: Parrot Sequoia Multi-Spectral Camera [7], [8]	48
Figure 34: DJI Mavic 3M (Multispectral Edition) (1)	51
Figure 35: STM32 Nucleo-F303RE Microcontroller [5]	53
Figure 36: Pinout for STM32 Nucleo-F303RE Microcontroller [5]	54
Figure 37: 2.10.2 Display: uLCD-144-G2 [6].....	54
Figure 38: Temperature & Humidity sensor - DHT-11 [7].....	55
Figure 39: pH Scale [11].....	56
Figure 40: Board Pin mapping [12]	56
Figure 41: MQ-135 Pin mapping [13]	57
Figure 42: LDR in voltage divider configuration.....	57
Figure 43: Soil Moisture Circuit	58
Figure 44 A raster dataset is composed of a matrix of pixels representing a geographical region, with each pixel connected to certain spatial information of that region [1]	61
Figure 45 Green.....	62
Figure 46 NIR	62
Figure 47 RED	62
Figure 48 REDGE.....	62
Figure 49 Calculation of NDVI with raster calculator in QGIS	62
Figure 50 NDVI result of analysis	63
Figure 51 Colour Ramp with corresponding NDVI values	64
Figure 52 Histogram on NDVI	64
Figure 53 NDWI calculated with QGIS	65
Figure 54 Histogram for NDWI	66
Figure 55: 2-DOF mmWave Sensors: TI's IWR1642BOOST (left) and Infenion's Distance2Go (right)	70
Figure 56: IWR1843BOOST Sensor	71

List of Tables

Table 1: Comparison of Technologies from Related Works.....	20
Table 2: Comparison of Commercially Available Cameras for Image Processing Applications	43
Table 3: Comparative Study of Commercially Available AI Cameras	47
Table 4: DJI Mavic 3M Specifications.....	51

1 Introduction to the Project

1.1 Concept and Objectives

The general objective of this project is the adaptation of existing technologies used in a precision agriculture (PA), into an indoor (greenhouse) prototype system which includes the use of both an unmanned ground and aerial vehicles (UGV and UAV). The term precision agriculture refers to the use of information technologies (IT) to help farmers manage the optimal growth of their crops thus ensuring profitability and sustainability. Furthermore, PA has also been known to help the environment by avoiding unnecessary spraying of pesticides as well as excessive use of water and fertilisers. The use of unmanned systems offers higher spatial resolution data compared to satellites. The real-time data of interest to the farmers and management tools/software includes soil properties such as moisture, compaction, salinity and nutrients (nitrogen (N), phosphorus (P) and potassium (K)), and crop monitoring which includes vegetation indexes such as Chlorophyll, Leaf Water, Ground Cover, Leaf Area, Normalised Difference Vegetation Index (NDVI), etc. UAVs have been used in PA for bird eye view, for insect identification using cameras and Lidars, and even actuators for autonomous spraying of pesticides, whereas the use of UGVs provides bottom-up capabilities identifying insects hiding under the leaves and for crop planting and harvesting. The innovation of this project is the UGV and UAV for indoor (greenhouse) PA applications where GPS signals are very weak or non-existent. In addition, this work will validate high-precision cm-level, 3D positioning techniques required for unmanned vehicle indoor localisation and navigation

1.2 Innovation and Originality

For many years, scientists and researchers with multidisciplinary backgrounds have been actively pursuing the utilization of unmanned systems for precision agriculture applications. However, most of the focus has been on outdoor applications mainly to satisfy the needs of farmers with vast farmland areas where a navigation accuracy in the range of 2-3 meters can be achieved using Global Navigation Satellite Systems (GNSS). None of the literature considers so far extending to indoor PA applications where GNSS performance and accuracy rapidly deteriorates. Worth noting that Cyprus greenhouse agriculture has been considered as “the most intensive and energy consuming horticultural systems”. Hence, this work proposes the implementation and testing of existing 2D and 3D indoor localization algorithms. With a cm-level accuracy then unmanned systems can be deployed in greenhouses to help farmers manage the optimal growth of their crops thus ensuring profitability and sustainability. Members of this project have extensive/expertise and track record of publications/research that demonstrates submeter-level accuracy in 2D and this project will be a unique opportunity to implement and test the performance of these algorithms for the demanding and dynamic application of indoor unmanned system navigation

Following the research trends in precision agriculture crop monitoring and vegetation indexes, we consider an image processing algorithm which utilizes a deep learning convolutional neural network. This algorithm will be an extension of

a newly developed system at the Inspire Research Center which accurately identifies fire, smoke, the types of atmospheric clouds as well as people and objects. The system is compact and lightweight that can easily be integrated on small UGV and UAV). The UGV and UAV will provide bottom-up and bird-eye views respectively of the vegetation. In addition, the UGV will be equipped with off-the-shelf sensors for soil humidity, pH and organic content which is essential data for the optimization process of irrigation and fertilization.

1.3 Added Value and Benefits

According to the Cyprus department of agriculture, the agricultural sector contributes 2,4% of the national GDP with the crop production contributing 35% of the total value added. On the other hand, Green Houses only occupy 0,5% of the total cultivated area, mostly because they are considered as the most intensive and energy consuming horticultural systems. Furthermore, according to the EU common agricultural policy (CAP) the first objective is to ensure a fair income to farmers and the second is to increase competitiveness. As reported for Cyprus for years 2005 to 2018, the agricultural income per worker is on average about 61% of the average wage in the whole economy, and also Cyprus has the lowest share of young farmers in the total number of farm managers in the EU in 2016 (1.3%).

This project aims towards the development of optimized outputs (irrigation, fertilization, pest control etc) which will significantly decrease the agricultural production costs in greenhouses. This competitiveness will promote the expansion of greenhouse use which will result in positive contributions towards farmers' wages, the national GDP and also attract the interest of young people to be involved.

Furthermore, high precision positioning is empowering additional life-changing applications such as emergency and natural disaster situations where wireless and the terrestrial networks are destroyed. UAVs and UGVs can serve as emergency platforms to provide wireless coverage for users and the first responders as well as video coverage for the emergency control centre. It is becoming evident that there is a more than ever need for high precision 3D positioning to empower the development of applications with very high economic and social impact and this project is expected to contribute towards this goal by adopting the most up-to-date positioning technologies to demonstrate and prove in the lab the feasibility of indoor unmanned system navigation and localization.

1.3.1 References

- [1] Cyprus Ministry of Agriculture, "Rural Development and the Environment", Online Posting: <https://moa.gov.cy/?lang=en> [Accessed 29/9/22].
- [2] European Commission Agricultural and Rural Development, "Key policy objectives of the new CAP", https://ec.europa.eu/info/food-farming-fisheries/key-policies/common-agricultural-policy/new-cap-2023-27/key-policy-objectives-new-cap_en [Accessed 29/9/22].

[3] European Commission Agricultural and Rural Development, “Cyprus Analytical Factsheet”https://ec.europa.eu/info/sites/default/files/food-farming-fisheries/by_country/documents/analytical_factsheet_cy.pdf [Accessed 29/9/22].

1.4 Aims and Objectives

1.4.1 Aim

Concerns among the EU member states as indicated by the EU common agricultural policy (CAP) is that farming competitiveness and farmers' income has declined and as a result so did the number of young people following the profession. In addition, Cyprus greenhouse agriculture has been considered as “the most intensive and energy consuming horticultural systems”. On the other hand, an abundance of literature shows that Precision Agriculture (PA) using Unmanned Ground and Aerial Vehicles (UGV and UAV) has helped farmers manage the optimal growth of their crops thus ensuring profitability and sustainability. However, for indoor applications, the bottleneck and Achilles heel of these technologies is the dependency on the navigation systems which rely purely on Global Navigation Satellite Systems (GNSS) whose performance rapidly deteriorates in satellite-obstructed environments. This opens research opportunities with engineers exploring new technologies such as Ultra-Wideband (UWB), millimetre-Wave (mmWave), antenna arrays and Internet of Things (IoT) aiming at sub-meter level accuracy. **DEMTRA will push the research envelope for indoor positioning by deploying state of the art 2D and 3D positioning algorithms for UGV and UAV navigation respectively.**

1.4.2 Technical Objectives

The vision of DEMTRA is to demonstrate the ability and applicability of unmanned systems for greenhouse/indoor 3D precision agriculture. For the vision to be achieved the following technical requirements have been set:

- TO1) Validate through measurements and assess the performance of the state-of-the-art 2D and 3D positioning techniques for Indoor UGV and UAV Navigation. This includes the setting up of experiments according to pre-defined scenarios to validate the existing techniques as reported in the literature and assess their performance against set KPIs. This also includes a sensitivity analysis of the techniques considering various environmental and other conditions. For example, the growing crops and vegetation inside the greenhouse will affect the positioning accuracy through multipath fading and signal strength variations. All these will have a direct effect on the positioning accuracy therefore a sensitivity analysis on the factors that affect the accuracy will be conducted.
- TO2) Validate the performance of the UAV multispectral imaging system capabilities. This includes the setting up of real-life experiments according to pre-defined scenarios to validate existing image processing algorithms as

reported in the literature and assess their performance against set KPIs. For instance, the robustness of the image processing algorithm when subjected to the UAV vibration interference conditions.

- TO3) Validate the performance of the UGV soil properties sensors: This includes the setting up of real-life experiments according to pre-defined scenarios to calibrate and validate the sensor measurements and assess their performance against set KPIs.
- TO4) Integrate the various subsystems to proof the concept of 3D Precision Agriculture.

1.4.3 *Operational Requirements*

For the aforementioned objectives to be achieved the following operational requirements have been set:

- OR1) Literature Review and State of the Art
 - Precision Agriculture
 - Smart Greenhouses
 - Image Processing Techniques and Algorithms for Insect Detection
 - Vegetation Indices
 - Indoor Positioning
 - Image Processing Techniques and Algorithms for Distance Calculation
- OR2) Market Research for Commercially Available Products
 - Cameras for Image Processing Applications
 - Sensors for Precision Agriculture Applications
 - Cameras for Distance Calculation
 - Multispectral Camera for Vegetation Index
 - Indoor Positioning Sensors
 - Unmanned Systems (Ground and Aerial)
- OR3) Purchase of identified sensors and equipment
- OR4) Setup up test-beds (prototypes) to collect related data
- OR5) Data Evaluation

2 Literature Review

2.1 Precision Agriculture Applications

Aerial systems used for agricultural applications date back to 1906 when seeds were spread over a swamp in New Zealand with the aid of a hot air balloon, but it was not until 1997 when an unmanned aerial vehicle (UAV) with Vertical Take-off and Landing (VTOL) capabilities, the Yamaha Rmax helicopter, was used for field spraying [1-3]. The high costs associated with the use of unmanned systems limited their use predominantly for military applications. However, advancements in technology and engineering over the last 20 years, have enabled the production of an abundance of sensors and unmanned systems, affordable for commercial applications. The list of such applications includes but it is not limited to aerial photography, search and rescue, inspection of power lines, survey of archaeological sites, etc, and in more recent years unmanned systems have been used extensively for agricultural applications also known as Precision Agriculture (PA). The term precision agriculture refers to the use of information technologies (IT) to help farmers manage the optimal growth of their crops thus ensuring profitability and sustainability. Furthermore, PA has also been known to help the environment by avoiding unnecessary spraying of pesticides as well as excessive use of water and fertilizers. The use of unmanned systems offers higher spatial resolution data compared to satellites. The real-time data of interest to the farmers and management tools/software includes soil properties such as moisture, compaction, salinity and nutrients (nitrogen (N), phosphorus (P) and potassium (K)), weather data (temperature and relative humidity), and crop monitoring which includes vegetation indexes such as Chlorophyll, Leaf Water, Ground Cover, Leaf Area, Normalized Difference Vegetation Index (NDVI), etc. UAVs have been used in PA for bird eye view, for insect identification using cameras and Lidars, and even actuators for autonomous spraying of pesticides, whereas the use of UGVs provides bottom-up capabilities identifying insects hiding under the leaves and for crop planting and harvesting. An extensive literature review is provided by review papers [1] and [4-12] which cite more than 1285 works whereas [13] alone cites 1318 related works. The importance of unmanned systems and agriculture is clearly indicated by their market share. According to Business Insider [14] the UAV market has surpassed \$12 billion in 2021 and more specifically the UAV market for agricultural applications based on Global Market Insights [15] is forecasted to exceed \$1 billion by 2024. Furthermore, concerns on climate change and the forecasted increasing global population by year 2050 reaching 10 billion, identify a mandatory increase on the production of agricultural goods in the range of 70% [16-17]. According to Allied Market Research [18], in the last 5 years, PA has been growing by 14.9% and is expected to reach \$7.8 billion by 2022.

PA incorporates the use of information technologies (IT) to help farmers manage the optimal growth of their crops thus ensuring profitability and sustainability. Derived from literature PA is best described with the following block diagram.

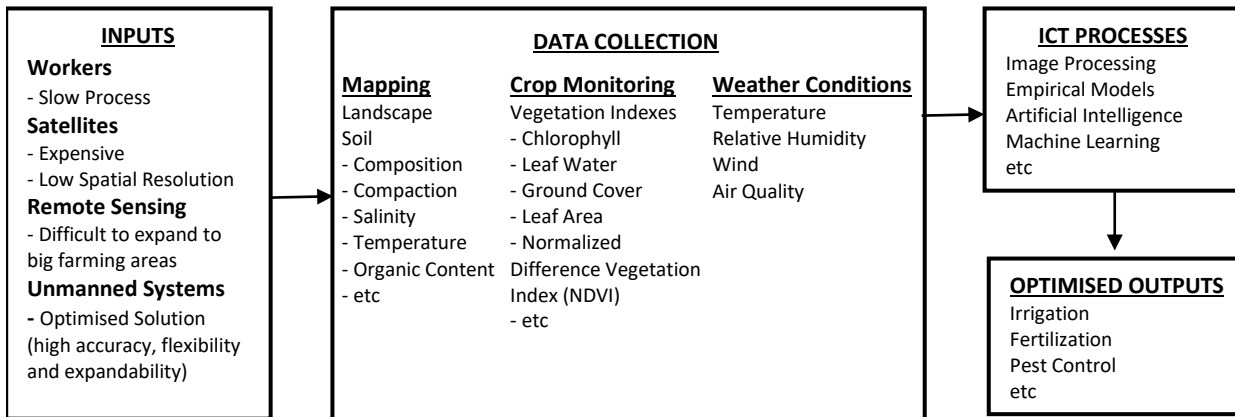


Figure 1: PA Block Diagram Derived from Literature

The extensive literature agrees that the use of unmanned systems provide a more optimized approach to precision farming. Most of the data collection can be achieved with the use of cameras (RGB, Thermal, NIR and Multispectral), Light Detection and Ranging (LiDAR), and there are also miniaturized specialized sensors for weather conditions as well as soil properties (composition, compaction, salinity, etc). Nowadays, there is an abundance of cameras and LiDARs ranging from 90 grams up to 1.3kg which enables the use of UAVs with low payload capabilities.

In the case of unmanned aerial vehicles, the preferred choice includes helicopters and/or multi-copters because of higher flexibility and maneuverability compared to fixed wing planes, whereas the use of unmanned ground vehicles adds an added valued towards planting, fertilizing, spraying and harvesting.

Finally, all the literature shows PA using unmanned systems limited to outdoor applications and none of the literature is for indoor (i.e., greenhouse) applications which would be beneficial for Cyprus. The bottleneck and Achilles heel of these technologies is the dependency on the navigation systems which rely purely on Global Navigation Satellite Systems (GNSS) whose performance rapidly deteriorates in covered areas.

2.1.1 References

- [1] del Cerro, J.; Cruz Ulloa, C.; Barrientos, A.; de León Rivas, J. Unmanned Aerial Vehicles in Agriculture: A Survey. *Agronomy* 2021, 11, 203. <https://doi.org/10.3390/agronomy11020203>.
- [2] Sugeno, M.; Hirano, I.; Kotsu, S. Development of an intelligent unmanned helicopter. In Proceedings of the 1995 IEEE International Conference on Fuzzy Systems, Yokohama, Japan, 14–20 March 1995; Volume 5, pp. 33–34.
- [3] Yamaha Motors, “Yamaha Rmax Helicopter”, Online Posting: <https://www.yamahamotorsports.com/motorsports/pages/precision-agriculture-rmax> [Accessed 9/8/21].
- [4] P. R. Grammatikis, P. Sarigiannidis, T. Lagkas and I. Moscholios, “A compilation of UAV applications for precision agriculture”, *Science Direct, Computer Networks* 172 (2020) 107148.

- [5] A. Otto , N. Agatz , J. Campbell , B. Golden , E. Pesch , Optimization approaches for civil applications of unmanned aerial vehicles (uavs) or aerial drones: a survey, Networks 72 (4) (2018) 411–458 .
- [6] J. Kim, S. Kim, C. Ju and H. I. Son, "Unmanned Aerial Vehicles in Agriculture: A Review of Perspective of Platform, Control, and Applications," in IEEE Access, vol. 7, pp. 105100-105115, 2019, doi: 10.1109/ACCESS.2019.2932119.
- [7] UM Rao Mogili, B B V L Deepak, "Review on Application of Drone Systems in Precision Agriculture", Procedia Computer Science, Volume 133, 2018, Pages 502-509, ISSN 1877-0509, <https://doi.org/10.1016/j.procs.2018.07.063>.
- [8] E. Raymond Hunt Jr. & Craig S. T. Daughtry (2018) What good are unmanned aircraft systems for agricultural remote sensing and precision agriculture? International Journal of Remote Sensing, 39:15-16, 5345-5376, DOI: 10.1080/01431161.2017.1410300.
- [9] Pasquale Daponte et al 2019 IOP Conf. Ser.: Earth Environ. Sci. 275 012022.
- [10] Pablo Gonzalez-De-Santos, Roemi Fernández, Delia Sepúlveda, Eduardo Navas and Manuel Armada, "Unmanned Ground Vehicles for Smart Farms", IntechOpen, Agronomy - Climate Change and Food Security, pp. 1-23, 2020, DOI: 10.5772/intechopen.90683.
- [11] Vu, Q., Raković, M., Delic, V., & Ronzhin, A. (2018). Trends in Development of UAV-UGV Cooperation Approaches in Precision Agriculture. Interactive Collaborative Robotics, 213–221. doi:10.1007/978-3-319-99582-3_22
- [12] P. Tokekar, J. Vander Hook, D. Mulla and V. Isler, "Sensor planning for a symbiotic UAV and UGV system for precision agriculture," 2013 IEEE/RSJ International Conference on Intelligent Robots and Systems, 2013, pp. 5321-5326, doi: 10.1109/IROS.2013.6697126.
- [13] C.F. Liew, D. DeLatte, N. Takeishi, T. Yairi, Recent developments in aerial robotics: a survey and prototypes overview, arXiv preprint: 1711.10085 (2017).
- [14] A. Meola, "Precision agriculture in 2021: The future of farming is using drones and sensors for efficient mapping and spraying", (Feb 8, 2021), Online Posting: <https://www.businessinsider.com/agricultural-drones-precision-mapping-spraying> [Accessed 9/8/21].
- [15] A. Bhutani, "Agricultural Drones Market worth over \$1 billion by 2024", (April 25, 2017), Online Posting: <https://www.gminsights.com/pressrelease/agricultural-drones-market> [Accessed 9/8/21].
- [16] G. Sylvester , E-Agriculture in action: drones for agriculture, Food and Agriculture Organization of the United Nations and International Telecommunication Union, Bangkok, 2018 .

- [17] M. C. Hunter, R. G. Smith, M. E. Schipanski, L. W. Atwood, and D. A. Mortensen, "Agriculture in 2050: Recalibrating targets for sustainable intensification," *Bioscience*, vol. 67, no. 4, pp. 386–391, 2017.
- [18] P. Bisht, J. Jayamon and E. Hira Allied Market Research, "Precision Agriculture Market", Online Posting: <https://www.alliedmarketresearch.com/precision-agriculture-market> [Accessed 9/8/21].

2.2 Smart Green Houses

Controlled plant growth has existed since the roman times, during which roman gardeners artificially grew cucumber-like vegetables every day. More specifically they planted the vegetables in wheeled carts and during the day they put them out in the sun but at night time they were taken inside. The first description of a greenhouse that used controlled temperature is in 1450s from a Korean cook book called Sanga Yorok. A traditional architecture called Ondol was used in this instance to artificially grow vegetables and assist in ripening the fruits. Ondols utilized a traditional underfloor heating system and cob walls to maintain heat and humidity and semi-transparent windows that allow sunlight infiltration whilst protecting the plants from the elements outside (Anon., 2021).

Greenhouses were initially referred to as botanical gardens which was later changed due to the introduction of the term “greenhouse effect”, describing the way a portion of the sun’s heat is absorbed by the earth’s atmosphere. Greenhouses work in a similar way, absorbing sunlight to warm up the structured area, which is why they are almost exclusively called “greenhouses” at this point (Hunt, 2021).

Greenhouses nowadays are structures used for plant growth in a controlled environment, with walls and roof made mostly out of transparent materials (usually glass) (figure 1). The equipment used in greenhouses includes actuators like heating, cooling, lighting and servos that are sometimes controlled by computers or microcontrollers. They are usually used to overcome issues short growing season or areas with poor sunlight and other environmental factors that affects negatively plant growth. In addition greenhouses allow specific crops that are seasonal to be cultivated throughout the year (Anon., 2021).

Considering that demand for food production is growing by the day, if the estimation that by 2050 the world population will reach 9.9 billion people (IISD, 2020), greenhouses will become more valuable. This is the reason why greenhouses should implement new technologies such as IoT, sensors and actuators in order to maximize the production efficiency will also minimizing the waste of resources and environmental pollution.

This is where “Smart Greenhouses” come into play. The main goal of a smart greenhouse is to maximize agricultural production while simultaneously maintain quality. Domestic greenhouse management today uses a more traditional and manual form of management for the most part, for example adjusting light, temperature, humidity and other parameters manually and based on experience. Smart greenhouses therefor can alleviate that with the usage of sensors and actuators that are more efficient, precise and also require less management costs (Li, et al., 2017).



Figure 2: Gothic Type Green House

A Smart Greenhouse, much like a regular greenhouse, creates a self-regulating microclimate optimal for plant growth through the usage of sensors, actuators and monitoring and control systems which enhance the plants growing conditions by atomizing the growth process (Ltd, 2021).

A fully functional unit for measuring and managing the internal environmental conditions of a greenhouse, was designed by Dr. Panos in February of 2021 (Fig. 3).



Figure 3: Dr. Panos's Smart-Greenhouse (Panos, 2021)

For the design of the specific smart greenhouse the components were an Arduino Uno, an Arduino Ethernet Rev.3, a DHT11 Temperature & Humidity sensor (4 pins), a DHT22 Temperature Sensor, an Ultrasonic Sensor – HC-SR04 (Generic), a DFRobot Gravity: Analog Soil Moisture Sensor, a Seed Grove – Gas Sensor (MQ2), a PIR Sensor (7m), an Axial Fan, a Brushless Motor, a Digilent 60W PCIe 12V 5A Power Supply and a DC Water Pump. The purpose of using this equipment is the monetarization and control, in real time, of the temperature, humidity, soil moisture and external environmental conditions through a smartphone application. Additionally, through controlled heating and cooling, fire and motion detection in the greenhouse and measurement of production growth, energy conservation can be achieved (Panos, 2021).

Avnet's Smart Greenhouse, is a system that was designed to support plant growth by monitoring energy consumption issues and providing a productive crop development under optimal conditions. This system operates by using a combination of IoT (Internet of Things), AI (Artificial Intelligence) and ML (Machine Learning) technologies in order to

attain an ideal greenhouse automation system. Moisture, pH, temperature, photometric, electrochemical and humidity sensors, CO₂ level and water, energy and photosynthesis meters are being used for the design of the Avnet's Smart Greenhouse. This combination of equipment offers real time diagnosis, optimal irrigation, remote management, reduction of harvest failures and information such as water and energy consumption and the fertility level of the soil (Company, 2021).

FarmRoad, Folium Wireless Multisensors (figure 3) is another example of a system being used in order to optimize the functionality of greenhouses.



Figure 4: Folium Wireless Multisensors (FarmRoad®, 2022)

It consists of battery-operated devices which aids producers to determine several problems that can occur in a greenhouse. Therefor multiple units form a single wireless sensor network that to offers environmental data at scale. To accomplish this each Folium is equipped with temperature, relative Humidity (RH), CO₂, PAR (Photosynthetically Active Radiation light sensor), RAD (Solar Radiation) Light, Barometric Pressure (BP), plant temperature and Soil/Substrate moisture sensors.

For the 4-sensor unit pack (Professional) the price is 3,997 dollars (3499.87 euro) and it includes 4 Folium multisensors units, 1-year software subscription (\$49/month/unit thereafter), free on boarding training and

A self-described smart and ubiquitous controlled-environment agriculture system called AgriSys focuses on sensors along the lines of air temperature, air humidity, soil moisture, soil PH, and light intensity. More specifically a temperature unit was utilized for the purpose of protecting the plans from either high or low temperatures. AgriSys also claims that it conserves water and decreases human power in agriculture (Abdullah, et al., 2016).

A group of university students, designed an intelligent management system for agricultural greenhouse based on the internet of things (IoT). The system includes temperature and humidity sensors, lighting, and irrigation equipment. Additionally, the system was designed to include a warning system and to operate from the network by using the ZigBee wireless communication network. All this equipment was devised to be managed by AT89C52 microcontroller (Li, et al., 2017).

Another system showcases an irrigation system for smart agriculture that is fully automated and is operated and monitored by an ARM9 (AT91SAM9G45) processor. This system monitors regularly the pH and nitrogen content in soil and can notify the user about temperature, moisture content and CO₂ percentage via the usage of the GSM module. The sensors used for the system are LM35 temperature sensor, SY-HS-220 humidity sensor and copper electrodes are used to determine the soil moisture. The system additionally makes use of a LCD controller, camera interface, audio, resistive touchscreen, Ethernet and high-speed USB and SDIO (Kavianand, et al., 2016).

Students from a department of computer science and technology in China, proposed an intelligent monitoring system for greenhouses that uses an android platform in order to monitor parameters (air temperature, moisture, soil temperature, CO₂ percentage) from mobile handsets. It promises real time video monitoring, maintenance and management from anywhere around the world will also being stable, cheap and easy to manage. The system makes usage of the advancement of wireless technology, microelectronics and wireless sensor networks. The wireless sensor network is based on ZigBee that has a bug scale, small volume and low cost and it provides the prospect of self-organizing, self-configuring and self-diagnosing which provides the remote management and monitoring (Liu, et al., 2017).

An IoT based Smart Greenhouse was proposed in 2016 by three Indian students. The irrigation system in this project uses an automatic drip irrigation that operates based on a specific soil moisture threshold set accordingly to an optimal amount of water required by the plants. The smart greenhouse also makes use of drip fertigation technics according to information from several minerals found in the soil. In addition foggers are also utilized to control temperature and humidity along with humidity and temperature sensors (Ravi , et al., 2016).

By using wireless communication technologies, another proposed smart greenhouse, connects a smart sensing system with a smart irrigation system by using a PLC. The system centres around parameters like soil moister content nutrient content and pH of the soil among the usual other parameters (temperature, light intensity, CO₂ percentage, and air humidity). This smart greenhouse consist of sensors, microcontrollers and a GSM module that provides communication. The sensors include moisture, spectroscopy, IR and opto-coupler sensors whilst the microcontroller used for the smart irrigation system specifically is the ATMEGA 328 (Chetan, et al., 2015).

Plenty greenhouse was launched in January 2020 in Larnaca, Cyprus and it covers 10,000 square meters of land accompanied with 85 square meters of store packaging facilities (Fig: 5).



Figure 5: Planty Greenhouse in Larnaca, Cyprus (Planty, 2020)

It uses a method called Nutrition film technique (NFT), which is a hydroponic method of growing plants. More specifically the roots of the plants are submerged in a shallow stream of re-circulating solution that contains essential minerals for optimal plant growth (Fig. 6).



Figure 6: Nutrition film technique (NFT) (Planty, 2020)

The facility also specializes in microgreens production using the Expanding Nursery Technique. Microgreens are very small vegetables that are 8 to 14 days old and just had their first leaves developed (Planty, 2020). The controller used in the facility is PLC (Programmable Logic Controller) that manages all the sensors and actuators, such as servos, heaters, coolers, lights, fans, temperature sensors, humidity sensors, pH sensors, etc.

Table 1: Comparison of Technologies from Related Works

Related Works	Controller & Sensors Used	Actuators Used	Type of the Connection	Result
1	<ul style="list-style-type: none"> • Arduino Uno • Arduino Ethernet (Rev.3) • DHT11 Temperature & Humidity sensor • DHT22 Temperature Sensor • Ultrasonic Sensor – HC-SR04 	<ul style="list-style-type: none"> • Axial Fan • Brushless Motor • Digilent 60W PCIe 12V 5A Power Supply • DC Water Pump 		<ul style="list-style-type: none"> • Monetarization and control, in real time, of the temperature, humidity, soil moisture and external environmental conditions through a smartphone application. • Through controlled heating and cooling, fire and motion detection in the

Related Works	Controller & Sensors Used	Actuators Used	Type of the Connection	Result
	<ul style="list-style-type: none"> DFRobot Gravity: Analog Soil Moisture Sensor Seed Grove – Gas Sensor (MQ2) PIR Sensor 		Wired	greenhouse and measurement of production growth, energy conservation can be achieved.
2	<ul style="list-style-type: none"> Moisture sensor pH meter Temperature sensor Photometric sensor electrochemical and humidity sensors CO2 level sensor Photosynthesis meter 	-	Wired & Wireless	<ul style="list-style-type: none"> Real time diagnosis Optimal irrigation Remote management Reduction of harvest failures Information such as water and energy consumption Fertility level of the soil
3	<ul style="list-style-type: none"> Temperature sensor Relative humidity sensor CC2 level sensor PAR (Photosynthetically Active Radiation light sensor) RAD (Solar Radiation) Light sensor Barometric Pressure (BP) sensor plant temperature sensor Soil/Substrate moisture sensors 	-	Wireless	<ul style="list-style-type: none"> Optimize the functionality of greenhouses Help in the determination of several problems that can occur in a greenhouse Offers environmental data at scale
4	<ul style="list-style-type: none"> Soil thermocouple sensor pH sensor Environmental temperature sensor Light sensor Soil moisture sensor 	<ul style="list-style-type: none"> Fan Pump Motor 	Wired	<ul style="list-style-type: none"> Conserves water usage Decreases required human power
5	<ul style="list-style-type: none"> Temperature sensor Humidity sensor Lighting sensor AT89C52 microcontroller 	<ul style="list-style-type: none"> Irrigation system ZigBee wireless communication network 	Wireless	<ul style="list-style-type: none"> Wireless monitoring Wireless warning system Wireless operation
6	<ul style="list-style-type: none"> ARM9 (AT91SAM9G45) processor pH meter Nitrogen meter Moisture sensor (copper electrodes) CO2 percentage meter LM35 temperature sensor SY-HS-220 humidity sensor 	<ul style="list-style-type: none"> GSM module LCD controller Camera interface Audio Resistive touchscreen Ethernet high-speed USB SDIO 	Wired & Wireless	<ul style="list-style-type: none"> The system consumes less water Less human power needed
7	<ul style="list-style-type: none"> Temperature sensor Humidity sensor Soil moisture sensor CO2 percentage meter Light sensor 	<ul style="list-style-type: none"> ZigBee Fan Lamp DC motor 	Wireless	<ul style="list-style-type: none"> Real time video monitoring Wireless maintenance & management Cheap Easy to manage Solar power supply
8	<ul style="list-style-type: none"> Intel Gen 2 Arduino Arduino IDE Ultrasonic Sensor Regrowing LED light RFID tag & sensor 	<ul style="list-style-type: none"> Peltier fan GSM sim900a LCD for display Relays Pumps Peltier Light Fogger 	Wired & Wireless	<ul style="list-style-type: none"> Uses an automatic drip irrigation Less human power needed It can be placed and operated on any given environment to grow any kind of vegetation Solar & wind energy source

Related Works	Controller & Sensors Used	Actuators Used	Type of the Connection	Result
9	<ul style="list-style-type: none"> • PLC • Microcontroller ATMEGA 328 • Moisture Sensor • Spectroscopic sensor • IR sensor 	<ul style="list-style-type: none"> • GSM module • Motor • IC L293 • Optocoupler 	Wired & Wireless	<ul style="list-style-type: none"> • Less human power needed • The system consumed less water
10	<ul style="list-style-type: none"> • PLC (Programmable Logic Controller) • Temperature sensors • Humidity sensors • pH sensors • etc 	<ul style="list-style-type: none"> • heaters • coolers • lights • servo • fan • etc 	Wired	<ul style="list-style-type: none"> • Conserves water usage • Decreases required human power • Easy to manage • Optimize the functionality of greenhouses • Help in the determination of several problems that can occur in a greenhouse

The literature review done for the purposes of the project helped focusing on the specific parameters that a greenhouse requires to monitor and adjust in order to successfully create an optimal microclimate for the plants. These parameters were narrowed down to temperature, humidity, carbon dioxide (CO₂), soil moisture, light intensity, water tank level and pH of the water. It additionally provided information about some of the commercially available products used in the greenhouses shown.

2.2.1 References

- [1] "WIKIPEDIA," 2021. [Online]. Available: https://en.wikipedia.org/wiki/Greenhouse#cite_note-2. [Accessed 29 11 2021].
- [2] G. Hunt, "greenhouse hunt," 2021. [Online]. Available: <https://www.greenhousehunt.com/faq/why-is-greenhouse-called-greenhouse/>. [Accessed 15 December 2021].
- [3] IISD, "World Population to Reach 9.9 Billion by 2050," IISD, 6 August 2020. [Online]. Available: <https://sdg.iisd.org/news/world-population-to-reach-9-9-billion-by-2050/>. [Accessed 25 November 2021].
- [4] Z. Li, J. Wang, R. Higgs, L. Zhou and W. Yuan, "Design of an Intelligent Management System for Agricultural Greenhouses Based on the Internet of Things," Beijing , Dublin, Qingdao, 2017.
- [5] FarmRoad®, "Folium Wireless Sensor Network," 2022. [Online]. Available: <https://www.farmroad.io/folium-greenhouse-multi-sensor>. [Accessed 11 4 2022].
- [6] Planty, "Our Story," 2020. [Online]. Available: <https://planty.eu/our-story/>. [Accessed 14 4 2022].

- [7] STMicroelectronics, "STM32 Nucleo-64 development board with STM32F303RE MCU, supports Arduino and ST morpho connectivity," 2022. [Online]. Available: <https://www.st.com/en/evaluation-tools/nucleo-f303re.html>. [Accessed 11 4 2022].
- [8] R. Elektronische, "uLCD-144-G2," 2021. [Online]. Available: <https://www.rutronik24.com/product/4d+systems/ulcd-144-g2/12405391.html>. [Accessed 11 4 2022].
- [9] adafruit, "DHT11 basic temperature-humidity sensor," 2020. [Online]. Available: <https://www.adafruit.com/product/386#description>. [Accessed 11 4 2022].
- [10] Components101, "DHT11-Temperature and Humidity Sensor," 2021. [Online]. Available: <https://components101.com/sensors/dht11-temperature-sensor>. [Accessed 11 4 2022].
- [11] S. Campbell, "HOW TO SET UP THE DHT11 HUMIDITY SENSOR ON AN ARDUINO," 2015. [Online]. Available: <https://www.circuitbasics.com/how-to-set-up-the-dht11-humidity-sensor-on-an-arduino/>. [Accessed 11 11 2022].
- [12] ©. E. Media, "NTC Thermistor," 2021. [Online]. Available: <https://eepower.com/resistor-guide/resistor-types/ntc-thermistor/#>. [Accessed 11 4 2022].
- [13] J. Consulting, "What is pH?," 2020. [Online]. Available: <https://www.jansanconsulting.com/ph-scale.html>. [Accessed 13 4 2022].
- [14] DFROBOT, "SKU:SEN0161-V2," 2018. [Online]. Available: https://wiki.dfrobot.com/Gravity__Analog_pH_Sensor_Meter_Kit_V2_SKU_SEN0161-V2. [Accessed 13 4 2022].
- [15] Q. components, "MQ-135 Air Quality Gas Sensor Module," 2022. [Online]. Available: <https://quartzcomponents.com/products/mq-135-air-quality-gas-sensor-module>. [Accessed 14 4 2022].
- [16] H. E. C. LTD, "TECHNICAL DATA MQ-135 GAS SENSOR," 2018. [Online]. Available: https://www.electronicoscaldas.com/datasheet/MQ-135_Hanwei.pdf. [Accessed 15 4 2022].
- [17] WebPlotDigitizer, "WebPlotDigitizer," 2021. [Online]. Available: <https://automeris.io/WebPlotDigitizer/>. [Accessed 15 4 2022].
- [18] k. O. Calculator, "Power regression Calculator," 2022. [Online]. Available: <https://keisan.casio.com/exec/system/14059931777261>. [Accessed 15 4 2022].

- [19] H. digital, “GL5516 Light Dependent Resistor LDR 5MM,” 2022. [Online]. Available: <https://www.hellasdigital.gr/electronics/sensors/light-and-color-sensors/gl5516-light-dependent-resistor-ldr-5mm/>. [Accessed 15 4 2022].
- [20] cactus.io, “How to Hookup Light Dependent PhotoResistor (LDR) to an Arduino,” 2019. [Online]. Available: <http://cactus.io/hookups/sensors/light/l dr/hookup-arduino-to-l dr-sensor>. [Accessed 15 4 2022].
- [21] “Anonymous,” 2021. [Online]. Available: https://en.wikipedia.org/wiki/Soil_moisture_sensor. [Accessed 17 4 2022].
- [22] skroutz, “SunLight SPA 12-9 Μπαταρία UPS με Χωρητικότητα 9Ah και Τάση 12V,” 2018. [Online]. Available: <https://www.skroutz.gr/s/8855346/SunLight-SPA-12-9-%CE%9C%CF%80%CE%B1%CF%84%CE%B1%CF%81%CE%AF%CE%B1-UPS-%CE%BC%CE%B5-%CE%A7%CF%89%CF%81%CE%B7%CF%84%CE%B9%CE%BA%CF%8C%CF%84%CE%B7%CF%84%CE%B1-9Ah-%CE%BA%CE%B1%CE%B9-%CE%A4%CE%AC%CF%83%CE%B7-12V.html#descript>. [Accessed 17 4 2022].
- [23] D. B. Ltd, “Designing Buildings,” 2021. [Online]. Available: https://www.designingbuildings.co.uk/wiki/Smart_greenhouse. [Accessed 08/11/2021 November 2021].
- [24] A. Khaldun I and F. A. Hint, “Design and Implementation a Smart Greenhouse,” International Journal of Computer Science and Mobile Computing , vol. 4, no. 8, p. 336, 2015.
- [25] D. Panos, “Project Hub,” 2021. [Online]. Available: <https://create.arduino.cc/projecthub/drpanosv/smарт-greenhouse-fbc739>. [Accessed 9 Novemper 2021].
- [26] A. Company, “/IOTCONNECT,” 2021. [Online]. Available: <https://www.iotconnect.io/smart-greenhouse-solution.html>. [Accessed 9 12 2021].
- [27] A. Abdullah, S. Al Enazi and I. Damaj, “AgriSys: A smart and ubiquitous controlled-environment agriculture system,” Salmiya, Kuwait, 2016.
- [28] G. Kavianand, M. V. Nivas, R. Kiruthika and S. Lalitha, “Smart drip irrigation system for sustainable agriculture,” Chennai, Tanjore, Chennai, 2016.
- [29] D. Liu, H. Wan, M. Zhang and J. Xiang, “Intelligent Agriculture Greenhouse Environment Monitoring System Based on the Android Platform,” Dailian, 2017.
- [30] K. K. Ravi , J. Vishal and K. Sumit, “IoT based smart greenhouse,” Warangal, 2016.

- [31] D. M. Chetan, R. R. Ganesh, S. Jagannathan and P. R, "Smart farming system using sensors for agricultural task automation," Chennai, 2015.
- [32] Yohkon, "Monocrystalline module YE6220M," 2020. [Online]. Available: <https://learn-eu-central-1-prod-fleet01-xythos.content.blackboardcdn.com/5d19e1c95e7e7/10437843?X-Blackboard-Expiration=1648684800000&X-Blackboard-Signature=hkk96Ycu1Xm%2F5g4SWIy3na%2F0WNh0QHGALJKtZbpsDM%3D&X-Blackboard-Client-Id=100100&response-cache-co>. [Accessed 31 3 2022].

2.3 Image Processing Algorithms for Small Unmanned System Applications

Climate change, has been responsible for the rapid increase of the size and frequency of forest/wild fires, which pose severe socioeconomic (the destruction of homes and loss of life) and environmental impact (carbon emissions, air and water quality) [1]–[5]. According to World Health Organization (WHO), 50% of recorded wildfires are from unknown origins and while the period between 1998-2017 affecting 6.2 million people and being responsible for 35,000 fatalities [6]–[8]. Other worldwide statistics report that wildfires were responsible for Australia's 2009 'Black Saturday' destruction of 1,800 homes and burnt area of 4,500 km² whereas in 2017, 10,200 structures and 5,559 km² in California, USA, and 4,180 km² in Portugal [9]. The cost of wildfires damage is typically between 10 to 50 times the suppression estimated worldwide to be more than \$100 billion annually [10].

Early warning methods and systems include the use of watchtowers, sensor networks, satellite remote sensing and patrolling using manned and unmanned aerial vehicles (UAVs). A comprehensive review of the aforementioned methods of early fire and smoke detection systems presented in [11] indicates that satellite systems provide a vast coverage area, but their response time depends on the location of the satellite and fire, while terrestrial sensor networks offer high accuracy and fast response times but their wide coverage is typically associated with significant increase in cost and system complexity. It seems that the use of small UAVs offers the highest future potential mostly because of their fast response time and extendable coverage area.

Advancements in technology and engineering over the last 20 years, have enabled the production of an abundance of sensors and unmanned systems, affordable for commercial UAV applications. The list of such applications includes but not limited to aerial photography [12], search and rescue [13], traffic monitoring [14], precision agriculture [15] and more. According to Business Insider [16] the UAV market has surpassed \$12 billion in 2021. Computer vision (image processing algorithms) using cameras has gained popularity in UAV applications. However, the cumbersome processing of real-time target detection algorithms, requires additional single board computers (SBC) to avoid possible interference with the navigation systems. Due to the strict run-time and payload availability on small and medium UAVs, the selection of onboard hardware is best addressed as a constraint optimization engineering process [17]. An elaborate comparison of the state of the art of commercially available SBC is examined by [18]. The study examined the UAV electrical power consumption due to the integrated SBC processing and its additional onboard weight. As concluded the Raspberry Pi (RPi) and Odroid platforms offer the lowest power consumption followed by the Jetson.

The aim of this work is the development of a fire detection system for small UAV applications. Taking into consideration the current research progress in deploying target detection algorithms on embedded devices, and hardware and practical considerations, the research objectives include: The development of a computer vision target detection algorithm with reduced false alarm rate that is able to run on a compact, lightweight, and cost-effective SBC, such as

RPi-4B while its performance is comparable to the state-of-the-art metrics (accuracy and real-time response) under real-life wildfire scenarios.

Ample of recent review papers [19]–[25] in fire detection and UAV applications, referencing more than 500 publications combined, conclude that convolutional neural networks (CNNs) which are a branch of deep learning algorithms, are currently achieving the best results in target detection and classification. Two-stage algorithms (R-CNN, Fast R-CNN, Faster R-CNN) [26]–[28] need to use the heuristic (selective search) or CNN network (RPN) to generate Region Proposal, and then do the classification and regression on Region Proposal. The other type of one-stage algorithms (YOLO, SSD) [29], [30], which uses only a CNN network to directly predict the class and location of different targets. The first method is more accurate but slower while the second algorithm is faster but less accurate. However, either networks usually require graphics processing units to operate properly because they are computationally challenging, use large amounts of memory, and are expensive to run. Therefore, deploying realtime target detection algorithms on SBC without powerful computing power is one of the current challenges of computer vision. Hence, works reported in the literature [31]–[33] examine the performance of "You Only Look Once" (YOLO) network which is becoming the most popular object detection model for SBC. As presented, the YOLO versions "tiny", offer higher inference speed (FPS) which however comes at a compromised reduced accuracy because of the reduced number of layers on the network. A successfully deployed YOLOv4 algorithm on a RPi platform achieving an improved inference speed to 2 FPS was reported in [34] while a YOLOv5 algorithm deployed on an unmanned aerial vehicle (UAV) for dynamic beehive detection and tracking achieving an inference speed of 0.5 FPS on RPi4 is reported in [35].

Nevertheless, this speed is still not fast enough for UAV applications, hence researchers began to experiment with deploying target detection algorithms on the NVIDIA Jetson Nano, at the expense of higher power consumption. An Improved YOLOv5 based Real-time Spontaneous Combustion Point Detection Method was proposed using "FPN + PAN" in the Neck layer of YOLOv5 algorithm to enhance the detecting the smoke or flame in early stage and achieved 7 FPS speed in real-time video stream on NVIDIA Jetson Nano [36]. Finally, the authors of [37] used a single-shot object detector based on deep convolutional neural networks (CNNs) deployed on Odroid-XU4 achieving 8-10 FPS with a accuracy around 95% and 5-6 FPS at 95% on a RPi3B. However, in both cases the CPU usage reached 100%.

2.3.1 References

- [1] H. Heidari, M. Arabi and T. Warziniack, "Effects of Climate Change on Natural-Caused Fire Activity in Western U.S. National Forests", *Atmosphere*, 981, 1-12, 2021.
- [2] J.E. Halofsky, D.L. Peterson and B.J. Harvey, " Changing wildfire, changing forests: The effects of climate change on fire regimes and vegetation in the Pacific Northwest, USA", *Fire Ecol.* 16, 1–26, 2020.

- [3] P. Gao, A.J. Terando, J.A. Kupfer, J. M Varner, M.C. Stambaugh, T.L.Lei and J. K. Hiers, "Robust projections of future fire probability for the conterminous United States", *Sci. Total Environ.* 789, 2021.
- [4] H. Heidari, T. Warziniack, T.C. Brown and M. Arabi, "Impacts of climate change on hydroclimatic conditions of US national forests and grasslands", *Forests* 139, 1-12, 2021.
- [5] W.S. Keeton, P.W. Mote and J.F. Franklin, "Chapter 13—Climate variability, climate change, and western wildfire with implications for the urban-wildland interface", *Adv. Econ. Environ. Resour.* 6, 225–253, 2007.
- [6] A. Vaughan, "Wildfire pollution linked to at least 33,000 deaths worldwide", *Health, New scientist*, Online Posting: <https://www.newscientist.com/article/2289547-wildfire-pollutionlinked-to-at-least-33000-deaths-worldwide/> [Accessed 27/10/22].
- [7] Statista 2022, "Most severe wildfires by number of fatalities worldwide between 1900 and 2021", Online Posting: <https://www.statista.com/statistics/267801/death-toll-due-to-wildfires/> [Accessed 27/10/22].
- [8] IQ Fire Watch, "Global Impacts of Wildfires – Damages, Losses, Costs and Effects", Online Posting: <https://www.iq-firewatch.com/risk> [Accessed 27/10/22].
- [9] World Wild Life, "Fire Management", Online Posting: <https://www.worldwildlife.org/stories/fire-management> [Accessed 27/10/22].
- [10] P. Howard, "The Cost of Carbon Project - Flammable Planet: Wildfires and the Social Cost of Carbon", Institute of Policy Integrity, NY University, School of Law, 2014.
- [11] Panagiotis Barmpoutis, Periklis Papaioannou, "A Review on Early Forest Fire Detection Systems Using Optical Remote Sensing," 11 November 2020. Online Posting: <https://doi.org/10.3390/s20226442>. [Accessed 16 November 2022].
- [12] H. Shakhatreh et al., "Unmanned Aerial Vehicles (UAVs): A Survey on Civil Applications and Key Research Challenges," in *IEEE Access*, vol. 7, pp. 48572-48634, 2019, doi: 10.1109/ACCESS.2019.2909530.
- [13] P. Petrides, C. Kyrou, P. Kolios, T. Theocharides, and C. Panayiotou. 2017. Towards a holistic performance evaluation framework for drone-based object detection. In 2017 International Conference on Unmanned Aircraft Systems (ICUAS). 1785–1793. <https://doi.org/10.1109/ICUAS.2017.7991444>
- [14] C. Kyrou, S. Timotheou, P. Kolios, T. Theocharides, and C. G. Panayiotou, "Optimized vision-directed deployment of UAVs for rapid traffic monitoring" IEEE International Conference on Consumer Electronics, ICCE 2018, Las Vegas, NV, USA, January 12-14, 2018. 1–6. <https://doi.org/10.1109/ICCE.2018.8326145>

[15] J. del Cerro et al., "Unmanned Aerial Vehicles in Agriculture: A Survey", *Agronomy*, 11, 203, 2021.

<https://doi.org/10.3390/agronomy11020203>.

[16] A. Meola, "Precision agriculture in 2021: The future of farming is using drones and sensors for efficient mapping and spraying", (Feb 8, 2021), Online Posting: <https://www.businessinsider.com/agriculturaldrones-precision-mapping-spraying> [Accessed 3/1/23].

[17] S. Ioannou, "Discrete Linear Constrained Multivariable Optimization for Power Sources of Mobile Systems", PhD Dissertation, Electrical Engineering, University of South Florida, November 2008.

[18] D. Hulens, J. Verbeke and T. Goedeme, "How to Choose the Best 'Embedded Processing Platform for on-Board UAV Image Processing?", 10th International Conference on Computer Vision Theory and Applications (VISAPP-2015), pages 377-386, 2015.

[19] Keiron O'Shea, Ryan Nash, "An Introduction to Convolutional Neural Networks," 26 November 2015. Online Posting: <https://arxiv.org/abs/1511.08458>. [Accessed 18 September 2022].

[20] F.M. Anim Hossain, Y. M. Zhang and M. A. Tonima, "Forest fire flame and smoke detection from UAV-captured images using fire-specific color features and multi-color space local binary pattern", *Journal of Unmanned Vehicle Systems*, 30 June 2020, <https://doi.org/10.1139/juvs-2020-0009>

[21] Y. Zhao, J. Ma, X. Li and J. Zhang, "Saliency Detection and Deep Learning-Based Wildfire Identification in UAV Imagery", *Sensors*, 18(3), 712, 2018. <https://doi.org/10.3390/s18030712>

[22] A. Ramachandrana and A. K. Sangaiah, "A review on object detection in unmanned aerial vehicle surveillance", *International Journal of Cognitive Computing in Engineering*, Volume 2, pp 215-228, 2021.

[23] F. Ahmed and M. Jenihhin, "A Survey on UAV Computing Platforms: A Hardware Reliability Perspective", *Sensors*, 22, 6286, 2022. <https://doi.org/10.3390/s22166286>

[24] M. Iqbal, C. Setianingsih and B. Irawan, "Deep Learning Algorithm for Fire Detection," 2020 10th Electrical Power, Electronics, Communications, Controls and Informatics Seminar (EECCIS), 2020, pp. 237-242, doi: 10.1109/EECCIS49483.2020.9263456.

[25] K. Manoj et al. "Smoke and Fire Detection using Deep Learning: A Review", *International Journal of Advanced Research in Science, Communication and Technology (IJARSCT)*, Vol. 2, Issue 1, November 2022.

- [26] Girshick, Ross, et al. "Rich Feature Hierarchies for Accurate Object Detection and Semantic Segmentation." 2014 IEEE Conference on Computer Vision and Pattern Recognition, June 2014. Crossref, <https://doi.org/10.1109/cvpr.2014.81>.
- [27] Girshick, Ross. "Fast r-cnn." In Proceedings of the IEEE international conference on computer vision, pp. 1440-1448. 2015.
- [28] Ren, Shaoqing, et al. "Faster r-cnn: Towards real-time object detection with region proposal networks." Advances in neural information processing systems 28 (2015).
- [29] Redmon, Joseph, et al. "You only look once: Unified, real-time object detection." Proceedings of the IEEE conference on computer vision and pattern recognition. 2016.
- [30] Liu, Wei, et al. "Ssd: Single shot multibox detector." European conference on computer vision. Springer, Cham, 2016.
- [31] H. Feng, et al., "Benchmark Analysis of YOLO Performance on Edge Intelligence Devices", Cryptography 2022, 6, 16. <https://doi.org/10.3390/cryptography6020016>
- [32] U. Nepal and H. Eslamiat, "Comparing YOLOv3, YOLOv4 and YOLOv5 for Autonomous Landing Spot Detection in Faulty UAVs", Sensors 2022, 22, 464. <https://doi.org/10.3390/s22020464>
- [33] M. E. Atik, Z. Duran and R. Ojgunluk, "Comparison of YOLO Versions for Object Detection from Aerial Images", International Journal of Environment and Geoinformatics (IJEGEO), Vol. 9, Issue 2, 2022.
- [34] Song Han, Huizi Mao, William J. Dally, "Deep Compression: Compressing Deep Neural Networks with Pruning, Trained Quantization and Huffman Coding", 15 February 2016. Online Posting: <https://arxiv.org/abs/1510.00149>. [Accessed 16 November 2022].
- [35] Wahyutama, A.B.; Hwang, M. YOLO-Based Object Detection for Separate Collection of Recyclables and Capacity Monitoring of Trash Bins. Electronics 2022, 11, 1323. [Accessed 16 November 2022].
- [36] Gao, P., Lee, K., Kuswidiyanto, L.W. et al. Dynamic Beehive Detection and Tracking System Based on YOLO V5 and Unmanned Aerial Vehicle. J. Biosyst. Eng. (2022). <https://doi.org/10.1007/s42853-022-00166-6>
- [37] C. Kyrkou, G. Plastiras, T. Theocharides, S. I. Venieris and C. S. Bouganis, "DroNet: Efficient convolutional neural network detector for real-time UAV applications", 2018 Design, Automation & Test in Europe Conference & Exhibition, 2018. doi:10.23919/date.2018.8342149

2.4 3D Positioning and Tracking Using AI Cameras

Indoor localization is significantly affected by the limitations of traditional techniques and algorithms which rely on the Global Navigation Satellite Systems (GNSS) whose accuracy deteriorates in sheltered areas. Advancements in technology and manufacturing engineering have enabled the expansion of Internet of Things (IoT) as well as miniature unmanned systems (UAS) which desperately need accurate indoor localization algorithms. This need reignited the interest of the research community to tackle this problem. Review papers [1] and [2] with more than 300 references provide an extensive comparison of the current state-of-the-art on 3D indoor positioning systems using radio frequency technologies (WiFi, UWB, mm-wave, etc) including geometric approaches like angle of arrival (AoA), time of arrival (ToA), time difference of arrival (TDOA), fingerprinting approaches based on Received Signal Strength (RSS), Channel State Information (CSI), Magnetic Field (MF) and Fine Time Measurement (FTM) as well as fusion-based and hybrid-positioning techniques. Additional approaches to indoor positioning are based on light (LIP – light based indoor positioning) where photo-diodes and/or cameras track the reflected visible or infrared light. Worth noting, that LIP systems are not affected by electromagnetic interference. An elaborate review of LIP systems is presented by [3]. Both LIP and RF technologies offer positioning accuracy in the centimeter (cm) range. However, none of the aforementioned technologies can provide object identification and tracking, hence opening a new area of research study.

Cameras have been successfully used for 3D indoor positioning applications using image processing techniques. In the area of medicine the use of a camera improved the “auto-positioning” accuracy in the mm-range by detecting the body contours for patients undergoing computed tomography (CT) [4]. In [5], a single camera was localized with an accuracy of 10mm in a known environment using the Perspective-n-Point (PnP) algorithm. However, as stated the accuracy depends on pre-computed 3D map of the environment which includes the 3D point clouds with co-registered intensity information. On the other hand, for unknown environments, indoor localization can be achieved using the Simultaneous Localization and Mapping (SLAM) algorithms [6-7]. For unknown environments, the depth information require the use of stereo or Time-of-Flight (ToF) cameras. As reported in [8] the indoor positioning of an unmanned aerial vehicle (UAV) was improved by 70% with the addition of a ToF camera as compared to the existing acoustic sensors.

Object identification and tracking requires the use of a stereo camera. In [9] an unmanned ground vehicle (UGV) with the use of camera could calculate the distance and azimuth from a preselected object whereas in [10] the 3D positioning of a moving object was estimated with an accuracy in the mm-range. Furthermore, Convolutional Neural Network (CNN) algorithms has shown to improve the image processing accuracy for 3D positioning in applications involving robotic localization [11-12] and also in industrial applications it improved worker safety, ergonomics and productivity [13].

In recent years, the most popular CNN algorithm for real time object detection is the YOLO (You Only Look Once) because it can be implemented on low power single board computers (SBC) [14-17]. An accuracy of 94% was achieved for Fire Localization in indoor and outdoor environments [18]. With a single camera, in outdoor environments, work

[19] identified and tracked a moving boat at a distance of 150m with an accuracy of 10m, whereas work [20] at a distance of 50m, identified and positioned a car with an accuracy of 2.5m. Furthermore, as reported in [21] at a distance of 20m, a car was positioned with an accuracy of 0.47m whereas a motorcycle with an accuracy of 0.62m. Theoretically, multi-camera implementation should achieve higher accuracy compared to single camera at the expense of higher processing requirements. However, work [22] using 2 cameras at a distance of 10m, reports an accuracy of only 4% which is equivalent to 0.4m. The same research identifies two major factors which significantly affect the accuracy of the results. First, is the distance between the cameras and second are the bounding boxes from each camera which might be considerably different. Similar, findings and conclusions are also given by [23].

2.4.1 *References:*

- [1] F. Zafari, A. Gkelias, and K. K. Leung, "A Survey of Indoor Localization Systems and Technologies". IEEE Communications Surveys & Tutorials, 1–1, 2019.
- [2] A Sesyuk, S Ioannou and M Raspopoulos, "A Survey of 3D Indoor Localization Systems and Technologies", Sensors 22 (23), 9380, 2022.
- [3] M. Maheepala, A. Z. Kouzani and M. A. Joordens, "Light-Based Indoor Positioning Systems: A Review", IEEE SENSORS JOURNAL, VOL. 20, NO. 8, APRIL 15, 2020.
- [4] R. Booij, R. P.J. Budde, M. L. Dijkshoorn and M. V. Straten, "Accuracy of automated patient positioning in CT using a 3D camera for body contour detection" Springer, European Radiology, Computed Tomography, 2018.
- [5] E. Deretey, M. T. Ahmed, J. A. Marshall and M. Greenspan, "Visual Indoor Positioning with a Single Camera Using PnP", 2015 International Conference on Indoor Positioning and Indoor Navigation (IPIN), 2015.
- [6] S. Grzonka, G. Grisetti and W. Burgard, "A Fully Autonomous Indoor Quadrotor", IEEE Trans. Robot. 28, 90–100, 2012.
- [7] M. T. Ahmed, M. Mohamad, J. A. Marshall, and M. Greenspan, "Registration of noisy point clouds using virtual interest points," in Proc. 2015 Canadian Conf. Computer and Robot Vision, ser. CRV '15, 2015.
- [8] J. A. Paredes, F. J. Álvarez, T. Aguilera nd J. M. Villadangos, "3D Indoor Positioning of UAVs with Spread Spectrum Ultrasound and Time-of-Flight Cameras", Sensors 18, 89, 2018.
- [9] C. T. Chao, M. H. Chung, J. S. Chiou and C.-J. Wang, "A Simple Interface for 3D Position Estimation of a Mobile Robot with Single Camera", Sensors, 16, 435, 2016.

- [10] A. Islam, M. Asikuzzaman, M. O. Khyam, M. Noor-A-Rahim and M. R. Pickering, "Stereo Vision-Based 3D Positioning and Tracking," in IEEE Access, vol. 8, pp. 138771-138787, 2020.
- [11] J. Miseikis, I. Brijacak, S. Yahyanejad, K. Glette, O. J. Elle and J. Torresen, "Multi-Objective Convolutional Neural Networks for Robot Localisation and 3D Position Estimation in 2D Camera Images," 2018 15th International Conference on Ubiquitous Robots (UR), pp. 597-603, 2018.
- [12] J. Miseikis et al., "Robot Localisation and 3D Position Estimation Using a Free-Moving Camera and Cascaded Convolutional Neural Networks," 2018 IEEE/ASME International Conference on Advanced Intelligent Mechatronics (AIM), pp. 181-187, 2018.
- [13] A. Munoz, A. Martí, X. Mahiques, L. Gracia, J. E. Solanes and J. Tornero, "Camera 3D positioning mixed reality-based interface to improve worker safety, ergonomics and productivity", CIRP Journal of Manufacturing Science and Technology Vol. 28, pp. 24-37, 2020.
- [14] H. Feng, et al., "Benchmark Analysis of YOLO Performance on Edge Intelligence Devices", Cryptography 2022, 6, 16. <https://doi.org/10.3390/cryptography6020016>
- [15] U. Nepal and H. Eslamiat, "Comparing YOLOv3, YOLOv4 and YOLOv5 for Autonomous Landing Spot Detection in Faulty UAVs", Sensors 2022, 22, 464. <https://doi.org/10.3390/s22020464>
- [16] M. E. Atik, Z. Duran and R. Ojgunluk, "Comparison of YOLO Versions for Object Detection from Aerial Images", International Journal of Environment and Geoinformatics (IJEGEO), Vol. 9, Issue 2, 2022.
- [17] J. Ye, S. Ioannou, P. Nikolaou and M. Raspopoulos, "CNN based Real-time Forest Fire Detection System for Low-power Embedded Devices", The 31st Mediterranean Conference on Control and Automation (MED2023), 2023.
- [18] R. R. Nori, R. N. Farhan and S. H. Abed, "Indoor and Outdoor Fire Localization Using YOLO Algorithm", J. Phys.: Conf. Ser. 2114 012067, 2021.
- [19] J. Wang, W. Choi, J. Diaz and C. Trott, "The 3D Position Estimation and Tracking of a Surface Vehicle Using a Mono-Camera and Machine Learning", Electronics, 11, 2141. 2022.
- [20] M. Vajgl, P. Hurtik and T. Nejezchleba, "Dist-YOLO: Fast Object Detection with Distance Estimation", Appl. Sci. , 12, 1354, 2022.
- [21] R. Waranusast, P. Riyamongkol and P. Pattanathaburt, "Distance Estimation Between Camera and Vehicles from an Image using YOLO and Machine Learning," 2022 Asia-Pacific Signal and Information Processing Association Annual Summit and Conference (APSIPA ASC), pp. 482-488, 2022.

[22] B. Strbac, M. Gostovic, Z. Lukac and D. Samardzija, "YOLO Multi-Camera Object Detection and Distance Estimation," 2020 Zooming Innovation in Consumer Technologies Conference (ZINC), pp. 26-30, 2020.

[23] G. Kulathunga, A. Buyval and A. Klimchik, "Multi-Camera Fusion in Apollo Software Distribution", IFAC-PapersOnLine Volume 52, Issue 8, Pages 49-54, 2019.

2.5 Indoor 3D Positioning Using mmWave Technology

Location-based services (LBS) are playing a critical role in our life for many years now, the most characteristic example being automotive navigation. While initially the need was for outdoor localization, very quickly this need has expanded in indoor or more generally in satellite-obstructed environments, where GNSS typically fail. There has been significant work reported in the literature [1] over the last 20-30 years which includes many solutions and approaches for solving the localization problem in satellite-denied environments using - over the years - the current available radio technologies, however none of these solutions has ever been standardized as the universal solution (like GNSS for outdoor) for this kind of environments. Someone could find various reasons for this, like the incremental need for more and more accuracy, the rapid evolution of wireless (and other) technologies that facilitate the support of this higher accuracy which makes the adoption of one system unreasonable if it is going to become obsolete soon, the cost and maturity of the underlying technologies to be integrated in mobile devices, etc. Moreover, localization accuracy is relatively subject to the application used. For instance, typical GPS-level accuracy (3-10m) would be sufficient for automobile navigation, room-level accuracy (2-4m) would be enough to identify the presence of someone in a room or area of an indoor environment. Nevertheless, modern smart applications and systems have imposed finer position accuracy requirements going down to sub-meter-level and in some very sophisticated applications down to cm-level accuracy. Literature reports many works for achieving meter-level accuracy [2, 1]. Most of these works adopt a geometric approach to estimate the location by typically utilizing radio-related context like the Received Signal Strength (RSS), the Time of Arrival (ToA), the Time Difference of Arrival (TDoA) and the Angle of Arrival (AoA). The accuracy of the estimated position is however subject to the accuracy of these signal parameters which depend on the characteristics of the underlying radio technology and most importantly on the bandwidth, the frequency, and the power of the transmission. Wider bandwidths allow for better resolution in the time domain and hence more accurate time resolution and thereafter more precise range and angle estimates to be measured which is then translated into a better positioning accuracy. The recent evolution of Ultra-Wideband (UWB) technology in conjunction with its deployment in modern smart devices made it attractive for reaching submeter-level accuracy and many works have already been reported in the literature. The wide bandwidth, although it becomes beneficial in terms of positioning accuracy, it limits the transmitted power and effectively the range and spatial coverage of UWB systems. For this reason, UWB has been established as the most suitable solution to provide sub-meter level accuracy only in open non-obstructed environments. The need is now shifting also towards obstructed environments and the accuracy requirement is going in some cases down to cm-level. In this context mmWave technology appears to be a more attractive option.

Millimetre-wave (mmWave) is defining a new era in modern wireless communication by providing very wide bandwidths. This technology is currently used in some Wi-Fi systems (e.g., IEEE802.11ad) and is planned to be used in 5G and 5G-beyond communications in the near future as the it offers much more flexibility to use wider bandwidths

and hence have the strong potential in achieving much higher data rates and capacity. mmWave systems typically operate in the frequency range between 30 to 300 GHz. The first standardized consumer radios were in the 60-GHz unlicensed band, i.e., 57–64 GHz, where 2-GHz signal bandwidth is typical in applications. The very large availability of bandwidth, together with the ease to use massive phase array antennas that allow the estimation of the azimuth and elevation angle can be used for achieving 3D cm-level accuracy or better [3]. Additionally, mmWave systems have higher transmit power allowance compared to UWB systems which compensates partly the high path losses typically experienced at high frequencies. The authors of [4] propose a multipath-assisted localization (MAL) model based on mmWave radar to perform indoor localization. The model considers the multipath effect when describing the characteristics of the reflected signal and precisely locates the target position by using the MAL area formed by the reflected signal. Experiments show that the model achieves a 3D positioning accuracy within 15cm. Also, the authors of [5] have demonstrated the benefits of array antennas towards identifying the orientation of the device. Although their work goes back to 2016, it is the very small wavelength at mmWave frequencies that facilitates the development of reasonably sized phased arrays that could aid the localization process by providing accurate angular information in 3D. Finally, due to this high sensitivity of the mmWave technology, positioning accuracy seems to be strongly correlated with the distance away from the target to be positioned. Positioning research using this mmWave technology is still on very early stages but early findings demonstrate its strong potential towards achieving the very high accuracy required by modern smart applications. The project aims to contribute towards these efforts by proving experimentally this concept and investigate the difficulties and challenges that need to be tackled.

Moreover, while, most of the works reported in literature focus in 2D, nowadays, smart applications have a 3D nature requiring the position to be estimated also in the z-dimension, making the need for 3D positioning even more predominant. Due to this, there is a growing research interest and activity during the last few years to develop/investigate positioning solutions in 3D. For example, the authors of [6] present a practical 3D position estimation method using an ankle-mounted sensing device, consisting of inertial measurement units (IMUs) and a barometer. Another work in [7] reports a 3D localization method for unmanned aerial vehicles (UAV) based on binocular stereovision technology is proposed.

It is evident that accurate localization systems are expected to play a pivotal role in the next generation of ICT technologies therefore it is a necessity to exploit the capabilities of mmWave technology towards achieving the desired accuracy. The 3D nature of the emerging applications also requires that this investigation is done in 3D. Therefore, the project aims to proof the applicability of mmWave towards achieving cm-level 3D positioning accuracy.

2.5.1 References

- [1] F. Zafari, A. Gkelias and K. Leung, "A Survey of Indoor Localization Systems and Technologies," IEEE Communications Surveys & Tutorials, vol. 21, no. 3, pp. 2568-2599, 2019.

- [2] C. Laoudias, A. Moreira, S. Kim, S. Lee, A. Wirola and C. Fischione, "A Survey of Enabling Technologies for Network Localization, Tracking, and Navigation," IEEE Communications Surveys & Tutorials, vol. 20, no. 4, pp. 3607-3644, 2018.
- [3] D. Wang, M. Fattouche and X. Zhan, "Pursuance of mm-Level Accuracy: Ranging and Positioning in mmWave Systems," IEEE Systems Journal, vol. 13, no. 2, pp. 1169-1180, 2019.
- [4] Hao, Z; et. al, "Millimetre-wave radar localization using indoor multipath effect," Sensors, vol. 22, p. 5671, 2022.
- [5] Y. Han, Y. Shen, X. Zhang, M. Z. Win and H. Meng, "Performance Limits and Geometric Properties of Array Localization," in IEEE Transactions on Information Theory, vol. 62, no. 2, pp. 1054-1075, Feb. 2016, doi: 10.1109/TIT.2015.2511778."
- [6] Y. Zhao, J. C. Y. Liang, X. Sha and W. Li, "Adaptive 3D Position Estimation of Pedestrians by Wearing One Ankle Sensor," IEEE Sensors Journal, vol. 20, no. 19, pp. 11642-11651, 2020.
- [7] S. Yu and e. Al., "A Low-Complexity Autonomous 3D Localization Method for Unmanned Aerial Vehicles by Binocular Stereovision Technology," in 10th International Conference on Intelligent Human-Machine Systems and Cybernetics (IHMSC), 2018.

2.6 Insects Present in Cyprus

All figures and details have been retrieved from EPPO (European and Mediterranean Plant Protection Organization) Global Database [1]. The database categorizes the organisms and monitors the 'spread of pests including invasive alien plants that damage cultivated and wild plants in agricultural and natural ecosystems. The database describes species of interest to agriculture providing scientific names, and geographical distribution, lists host plants, and provides a categorization of pests to monitor their presence and effect. The user can filter and browse the database by choosing the country of interest and status (i.e. absent, present, restricted distribution). For instance, Figure 7 - Figure 12 are images to present Spodoptera littoralis (SPODLI). The datasheet which involves information for detection and identification, biology, pest significance, and phytosanitary measures also contributed for each species. Spodoptera littoralis is found to damage cotton groundnuts, rice, cucurbitaceous vegetables, potatoes, and sweet potatoes in glasshouses. Insects viruses, and symptoms images included in this report have been listed as present and widespread in Cyprus in the database as of 1/11/2024.



Figure 7 *Spodoptera littoralis*(SPODLI)



Figure 8 *Spodoptera littoralis* (adult)

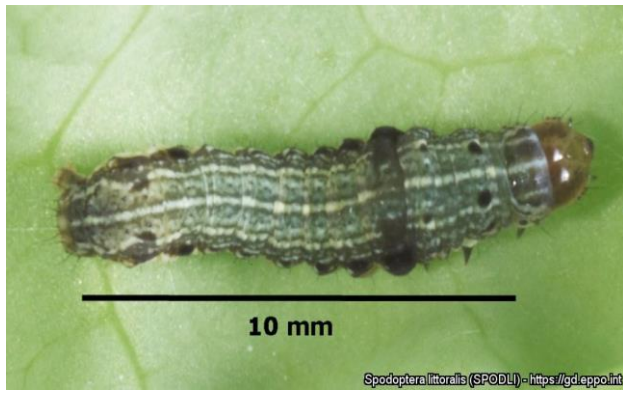


Figure 9 Early 3rd instar



Figure 10 Fully grown larva



Figure 11 Egg cluster on chrysanthemum.



Figure 12 4th instar.



Figure 13 *Atherigona orientalis* adult, dorsal view



Figure 15 *Atherigona orientalis* late stage damage of pepper fruits



Figure 14 cucumber mosaic virus



Figure 16 Cucumber mosaic virus on chilli pepper



Figure 17 *Comstockaspis perniciosus*



Figure 18 *Comstockaspis perniciosus* infestation on apple branch



Figure 19 *Liriomyza huidobrensis*



Figure 20 Leaf mines on *Liriomyza huidobrensis*



Figure 21 Symptoms of Pepino mosaic virus on cherry tomatoes



Figure 22 Leaf blistering symptoms from Pepino mosaic virus(PEPMV0)

2.6.1 References

- [1] EPPO (European and Mediterranean Plant Protection Organization) Global Database Online Posting:
https://www.eppo.int/RESOURCES/eppo_databases/global_database [Accessed 11/1/2024].

2.7 Commercially Available Cameras for Image Processing Applications

There are many cameras that are commercially available. The listed cameras are suitable for computer vision-based applications. As seen from table 2, these products come in various shapes and sizes. The product characteristics tabulated on Table 2 where either obtained or derived from the product datasheets. Only the important characteristics for small sized unmanned applications have been include in the analysis.



Figure 23: AVIOTEC IP Starlight 8000 Video-Based Fire Detection. (Bosch, 2016)



Figure 24: Fixed-Mount Thermal Camera FLIR A50/A70 Smart Sensor. (FLIR, 2022)



Figure 25: SR7FIRE-MD-DUAL system (thermal visible camera) for fire detection on industrial environment.



Figure 26: OAK SoM for depth and AI processing

Table 2: Comparison of Commercially Available Cameras for Image Processing Applications

Product	Compression	Max FPS and Resolution	Weight (kg)	Dimensions (mm)	Power Requirements	Price (US\$)
Bosch AVIOTEC FCS-8000-VFD-B	H.264, MJPEG	30fps at 1080P	0.855	78 x 66 x140	12V, 9W	4,563.25
FLIR A50/A70	H.264, MPEG4, MJPEG	30fps at 1280 x 960	NA	NA	24/48V, 8W	7,299.00
SR7FIRE-MD-DUAL system (thermal visible camera)	H.264/MPEG-4 & MJPEG	25fps at 1080P	NA	NA	12V, 9W	22,598.56
Luxonis OAK-D for depth and AI processing	H.264, H.265, MJPEG	60fps at 1080P	0.115	110x54.5x33	5V, 7.5W	249.00

The computer vision-based flame detection systems tabulated on Table 2 are highly accurate in detecting fire in real time. It is impressive that all systems consume lower than 10W of electric power while offering HD quality picture for processing. However, the SR7FIRE-MD-DUAL system (thermal visible camera) is very expensive and cannot be afforded by this

proof of concept project. In addition both SR7FIRE-MD-DUAL system and the FLIR A50/A70 even though their weight characteristics are not reported yet they look heavy and they are not suitable for small unmanned system applications.

In conclusion, the fourth option is the most suitable for small unmanned applications since its weight it is only 0.115kg, its price is only 249 US\$ and finally it is also suitable for distance measurements.

2.7.1 References

- [1] Bosch AVIOTEC IP STARLIGHT 8000 (FCS-8000-VFD-B), “Video-based fire detection”, Online Posting: <https://commerce.boschsecurity.com/us/en/Video-based-fire-detection/p/F.01U.317.536/> [Accessed 1/6/23].
- [2] Bosch AVIOTEC IP STARLIGHT 8000, “FCS-8000-VFD-B - Datasheets”, Online Posting: https://resources-boschsecurity-cdn.azureedge.net/public/documents/AVIOTEC_IP_starlight_Data_sheet_elGR_20875957771.pdf [Accessed 1/6/23].
- [3] FLIR A50/A70 Smart Sensor, “Model: 89995-0101-T300389 - Datasheets”, Online Posting: https://www.flir.eu/products/a50_a70-smart-sensor/?vertical=rd+science&segment=solutions [Accessed 1/6/23].
- [4] SR7FIRE-MD-DUAL SYSTEM, “Datasheet - SR7FIRE-MD-DUAL system (thermal visible camera)”, Online Posting: <https://www.sevecu.com/term-68-detail> [Accessed 1/6/23].
- [5] Luxonis OAK-D for depth and AI processing, “Hardware specifications”, Online Posting: <https://docs.luxonis.com/projects/hardware/en/latest/pages/BW1098OAK/> [Accessed 1/6/23].

2.8 Commercially Available Spectral Cameras for Small Unmanned System Applications

For precision agriculture applications, both multispectral and hyper-spectral cameras are used. Both technologies capture images with higher spectral resolution compared to what the human eye can see (color perception). Hyper-spectral cameras offer higher spectral resolution compared to multispectral cameras. Spectral resolution is the number of bands they record and how narrow the bands are. Hyper-spectral cameras have more than 100 bands, whereas multispectral ones have considerably less.

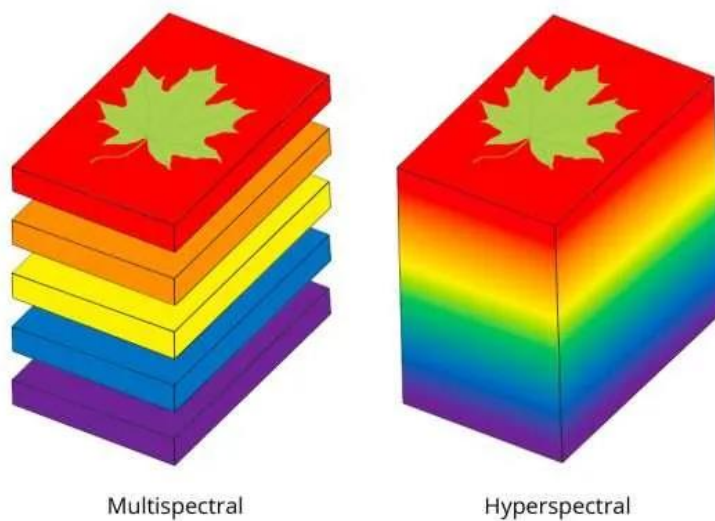


Figure 27: Hyperspectral vs. Multispectral data [1]

As nicely presented by Figure 27, a hyperspectral camera provides smooth spectra. The spectra provided by multispectral cameras are more like stairs or saw teeth without the ability to depict acute spectral signatures [1].

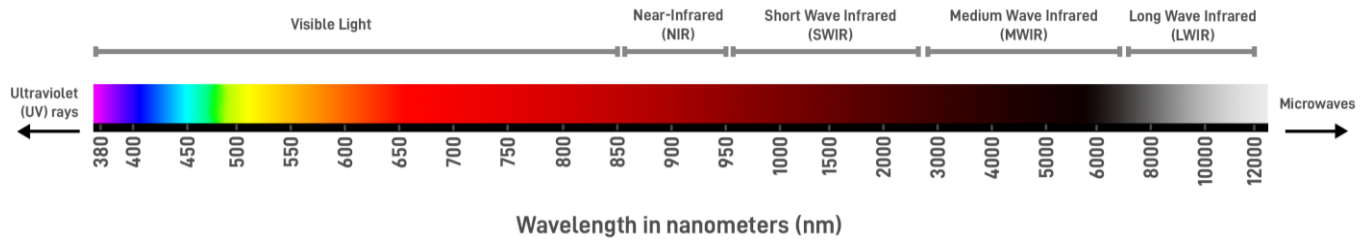


Figure 28: Visible and IR light spectrum [2]

Infrared imaging is generally very effective for obtaining visual detail below the surface of an object. It's proved incredibly useful in machine vision as it's possible to obtain information that just isn't viable using visible light. On the

other hand, Short wave Infrared (SWIR) imaging is commonly applied in order to perform tasks such as identifying bruising in fresh produce such as fruit and vegetables, defect identification in silicon items, and detecting different types of plastic in waste and recycling industries [2].

From figures 28 and 29, it can be derived that the band wavelengths are as followed:

- BLUE Band 3 (0.45-0.51 um)
- GREEN Band 2 (0.53-0.59 um)
- RED Band 1 (0.64-0.67 um)
- NEAR INFRARED (NIR) Band 5 (0.85-0.88 um)
- SHORT-WAVE INFRARED (SWIR 1) Band 4 (1.57-1.65 um)
- SHORT-WAVE INFRARED (SWIR 2) Band 4 (2.11-2.29 um)

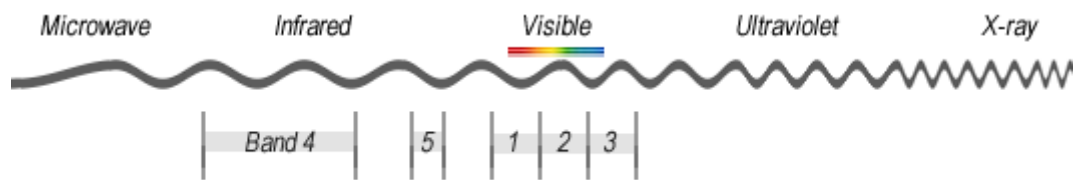


Figure 29: Wavelength and Band Allocation [3]

On the other hand, Hyperspectral images compared to multispectral ones, consists of hundreds or thousands of much narrower bands as shown on Figure 30. The band width could be as narrow as 10 to 20 nm.

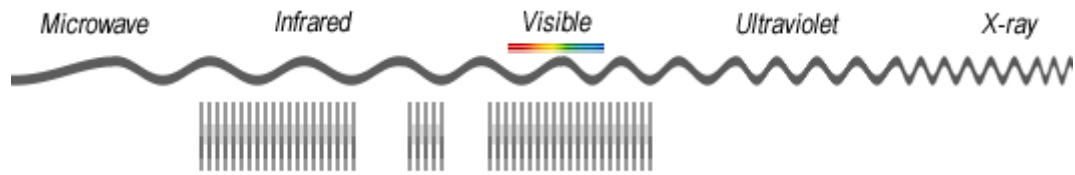


Figure 30: Hyperspectral Narrower Bands [3]

However, having the experience from the cameras for image processing presented in section 2.7, the price was the number one requirement for selecting a multispectral camera for the DEMETRA project. After an extensive online survey the following findings are reported as follows:

Table 3: Comparative Study of Commercially Available AI Cameras

Camera	Characteristics	Price	Suitability for DEMETRA Project	
			Advantages	Disadvantages
UAVfordrone [4]	Hyperspectral camera with DJI M300 Drone	US\$29,900 (incl. Educ. Discount)	<ul style="list-style-type: none"> • Hyperspectral Cam • Complete System including UAV 	Not Affordable
Headwall Photonics [5]	Hyperspectral Camera with analysing software	US\$ 100,000	Hyperspectral Cam	Not Affordable
Imec HIS [6]	Hyperspectral Camera with analysing software	€18,000 (incl. Educ. Discount)	Hyperspectral Cam	Not Affordable
Parrot Sequoia [7][8]	Multispectral Camera 4 Bands: 550 – 790nm	€3,500	Affordable	<ul style="list-style-type: none"> • It is approaching End of Life • Price does not include a UAV
Micasense RedEdge-P [8][9]	Multispectral Camera 5 Bands 475nm – 872nm	€8,000 Price does not include a UAV	5 Bands 475nm – 872nm	<ul style="list-style-type: none"> • Not Affordable
DJI Mavic 3M (DJI Mavic 3 Multispectral Edition) [8][10]	Multispectral camera including DJI Mavic 3M Green (G): 560 ± 16 nm; 4 Bands Green (G): 560 ± 16 nm Red (R): 650 ± 16 nm; Red Edge (RE): 730 ± 16 nm; Near infrared (NIR): 860 ± 26 nm;	€4,750 for complete system and delivery charges	Affordable	<ul style="list-style-type: none"> • 4 bands instead of 5

UAVforDrone



Figure 31: Hyperspectral camera with DJI M300 Drone [4]



Figure 32: Nano HP (400-1000nm) Hyperspectral Imaging Package [5]



Figure 33: Parrot Sequoia Multi-Spectral Camera [7], [8]

Some commercially available hyper-spectral and multispectral cameras and unmanned aerial systems are presented by Figures 31 to 33 and a bigger selection is presented on Table 3. The results of the comparative study of commercially available products that are tabulated on Table 3, show that hyper-spectral cameras are not affordable for the DEMETRA project which has a budget of €40,000. Hyperspectral camera solutions including educational discounts are exceeding €18,000 which is equivalent to 45% of the project budget.

On the other hand multispectral camera solutions are affordable and feasible with available prices being below €8,000. Parrot Sequoia multispectral camera is the cheapest solution at a price of €3,500. It offers 4 spectral bands in the range of 550 – 790nm but it is approaching its end-of-life. On the other hand, Micasense RedEdge-P offers 5 bands in the range of 475nm – 872nm at a higher than double cost of €8,000.

Finally, DJI offers a complete solution of a UAV with a multispectral camera, the DJI Mavic 3M (DJI Mavic 3 Multispectral Edition) at a total cost of €4,750. The multispectral camera offers only 4 bands. However, the spectral range of 650 to 860 is comparable to the other solutions.

Therefore, after an extensive comparison and analysis it was concluded that for the purposes of the DEMETRA project, the DJI Mavic 3M (DJI Mavic 3 Multispectral Edition) is the best solution. It is a complete system including a UAV and a multispectral camera at an affordable price.

2.8.1 References

- [1] Specim – A Konica Minolta Company, “HYPERSPECTRAL VS MULTISPECTRAL CAMERAS: UNDERSTANDING ADVANTAGES AND LIMITATIONS IN SPECTRAL IMAGING”, Online Posting: <https://www.specim.com/technology/hyperspectral-vs-multispectral-cameras/> [Accessed 1/6/23].
- [2] Clear View, “Non-Visible Imaging: Short-Wave Infrared (SWIR)”, Online Posting: <https://www.clearview-imaging.com/en/blog/non-visible-imaging-short-wave-infrared-swir> [Accessed 1/6/23].
- [3] GISGeography, “Multispectral vs Hyperspectral Imagery Explained”, Online Posting: <https://gisgeography.com/multispectral-vs-hyperspectral-imagery-explained/> [Accessed 1/6/23].
- [4] Drone for Agriculture, “Hyperspectral Camera and DJI M300”, Online Posting: <https://www.uavfordrone.com/> [Accessed 1/6/23].
- [5] Headwall Photonics, “Hyperspectral Imaging Systems & Spectroscopy Components for Fast, Actionable Results”, Online Posting: <https://headwallphotonics.com/> [Accessed 1/6/23].

[6] Imec HIS, “Hyperspectral imaging”, Online Posting: <https://www.imec-int.com/en/hyperspectral-imaging> [Accessed 1/6/23].

[7] The University of Edinburg, “AIRBORNE RESEARCH AND INNOVATION”, Online Posting: <https://www.ed.ac.uk/airborne/airborne-geosciences/airborne-sensors/multispectral-imaging/parrot-sequoia> [Accessed 1/6/23].

[8] Geosense, “Multispectral Cameras - Parrot Sequoia”, Online Posting: <https://www.geosense.gr/spectral-cameras/> [Accessed 1/6/23].

[9] AgEagle Aerial Systems Inc., “SENSORS MicaSense series”, Online Posting: <https://ageagle.com/solutions/micasense-series-multispectral-cameras/> [Accessed 1/6/23].

[10] DJI Agriculture, “DJI Mavic 3M”, Online Posting: <https://ag.dji.com/mavic-3-m/specs> [Accessed 1/6/23].

2.9 Commercially Available UAV for DEMETRA Project

As concluded in section 2.8, for the purposes of the DEMETRA project, the DJI Mavic 3M (DJI Mavic 3 Multispectral Edition) was the best solution. It is a complete system including a UAV and a multispectral camera at an affordable price. In this section we will examine the technical characteristics of the DJI 3M UAV. The characteristics were either derived or directly obtained from the product datasheets [1].



Figure 34: DJI Mavic 3M (Multispectral Edition) (1)

Table 4: DJI Mavic 3M Specifications

Weight (kg)	Dimensions (mm)	Max Flight Time (without wind)	RGB Camera
0.951	347.5×283×139.6	43 minutes	Single shot: 20 MP Timelapse: 20 MP
Multispectral Camera	Gimbal	RTK Module	Image Transmission System
Green (G): 560 ± 16 nm; Red (R): 650 ± 16 nm; Red Edge (RE): 730 ± 16 nm; Near infrared (NIR): 860 ± 26 nm;	Tilt: -135° to 45° Roll: -45° to 45° Pan: -27° to 27°	Fixed RTK: Horizontal: 1 cm + 1 ppm; Vertical: 1.5 cm + 1 ppm	2.400-2.4835 GHz 5.725-5.850 GHz

As shown from the technical characteristics tabulated on Table 3, the DJI is compact and light weight. With a total weight of nearly 1kg and diagonal dimensions of 38cm it is very convenient to fly inside green houses. In addition it is fully

equipped not only with the multispectral camera but with an additional RGB camera and both are stabilised by a 3-axis gimbal system and communication technologies for control and data transfer.

2.9.1 *References*

- [1] DJI Agriculture, “DJI Mavic 3M”, Online Posting: <https://ag.dji.com/mavic-3-m/specs> [Accessed 1/6/23].

2.10 Commercially Available Sensors for Greenhouse Applications

The literature review of smart greenhouses presented in section 2.2, including some additional references on sensor technologies and the importance measured data for agricultural applications, revealed the necessity of the following measured parameters; Air temperature, Air humidity, Sunlight, Carbon dioxide, Soil moisture and Mineral soil composition [1]-[4].

Greenhouses offer controlled environmental conditions hence crop cultivation is achieved and optimized by avoiding extreme temperatures, under and over watering, as well as lack of nutrients on the soil. In addition, the importance of sunlight, carbon dioxide and soil moisture relates to the process of photosynthesis where plants use to synthesize nutrients from carbon dioxide and water.

The project coordinator has extensive experience in electronics and sensor integration for various applications including wearable devices. Hence, from experience the following solutions were proposed to meet the project requirements.

2.10.1 Controller: STM32 Nucleo-F303RE Microcontroller

The STM32 Nucleo-F303RE (Fig. 35) is an easy to use microcontroller that has an integrated ST-Link/v2-1, used for the programming under mbed environment. The board can operate with 5 to 15 Volts and has a flexible power-supply options like ST-Link, USB Vbus or external sources. It has the Arm cortex M4 core that is clocked at 72MHz.

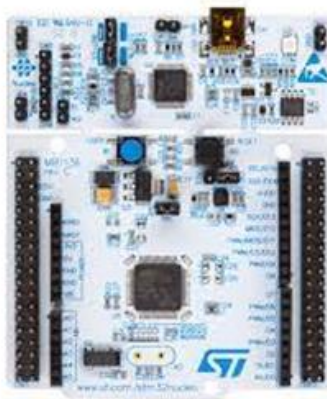


Figure 35: STM32 Nucleo-F303RE Microcontroller [5]

Looking closely to the F303 microcontroller pinout on Figure 36, it can be seen that it has numerous analogue and digital inputs and can supports communication protocols such as RS-232, I²C which are required for sensor integration. In addition, multiple pulse width modulation (pwm) digital outputs can accommodate actuators (servos, fans, relays, etc) which are required for starting and stopping the watering process, opening and closing windows and fans for temperature control etc.

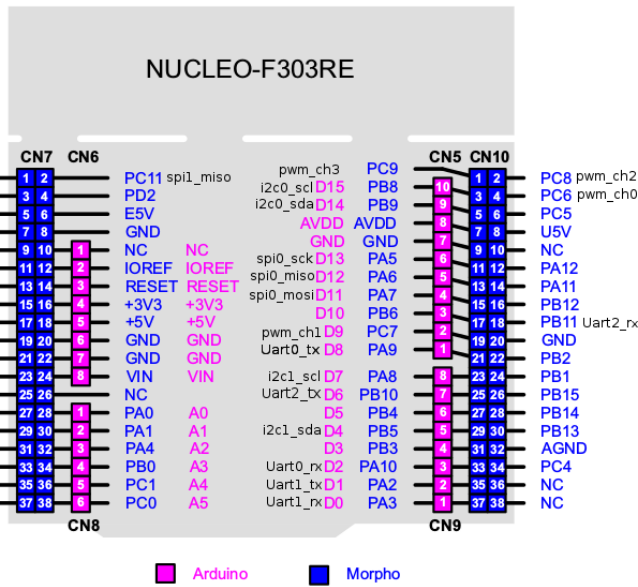


Figure 36: Pinout for STM32 Nucleo-F303RE Microcontroller [5]

This microcontroller can nicely serve the needs for this project because it supports all the necessary communication protocols and has ample ports that were needed for the required sensors and actuators.

2.10.2 Display: uLCD-144-G2

Monitoring systems need the integration of displays for outputting the measured data as well as for troubleshooting. For these purposes the uLCD-144-G2 screen is proposed. It is a colored and compact monitor; 1.44 inch screen, 52mm wide and 77mm long. The operating voltage is between 4.5V and 5.5V, and it communicates with the microcontroller via serial communication protocol [6].



Figure 37: 2.10.2 Display: uLCD-144-G2 [6]

2.10.3 Temperature & Humidity sensor - DHT-11

The DHT-11 is a small size, low power digital temperature and humidity sensor. It has 15.5mm x 12mm x 5.5mm of body size and is working with 3 to 5V power with a maximum current up to 2.5mA. It has 5% accuracy for 20 to 80% of humidity and $\pm 2^{\circ}\text{C}$ accuracy for 0-50°C of temperature. The sensor uses a capacitive humidity sensor and a thermistor

to measure the surrounding air. In addition the DHT-11 sensors contains a chip that does analog to digital conversion and exports a digital signal on the data pin that can be used for reading the temperature and humidity [7].

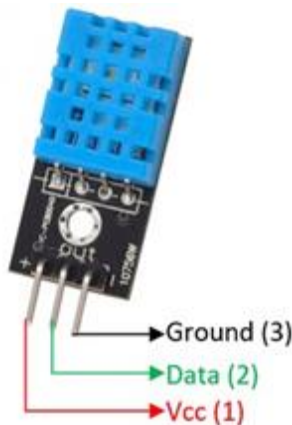


Figure 38: Temperature & Humidity sensor - DHT-11 [7]

The pinout mapping of the DHT-11 temperature and humidity sensor are presented on Figure 38. The sensor uses just one signal wire to transmit data to the microcontroller (pin 2). It is powered by pin1 with 3.3 or 5V and ground wires by pin 3. A 10K Ohm pull-up resistor is needed between the signal line and voltage line to make sure the signal level stays high by default.

The DHT11 measures the electrical resistance with a moisture holding substrate component between two electrodes to detect water condensation. When the water vapor is absorbed by the substrate, ions are discharged by the component which increases the conductivity between the electrodes. The change in resistance between the two electrodes is proportional to the relative humidity. Higher relative humidity decreases the resistance between the electrodes, while lower relative humidity increases the resistance between the electrodes [8].

The DHT11 measures temperature with a surface mounted NTC temperature sensor (theristor) built into the unit. NTC (Negative Temperature Coefficient) is a resistor with a negative temperature coefficient, in other words, the resistance decreases when the temperature rises. They are primarily used as resistive temperature sensors and current-limiting devices. NTC sensors are typically used in a range from -55 to 200 °C [9-10].

2.10.4 pH Sensor - SEN0161-V2

SEN0161-V2 is an analog pH meter that is designed to measure the pH of a liquid and reflect it is acidity or alkalinity. The onboard voltage regulator chip supports the wide voltage supply of 3.3-5.5V voltage availability of the main control board. The output signal is filtered by hardware and has low overall jitter and it has ± 0.1 measurement accuracy at 25°C.

The pH test is a scale of hydrogen ion activity in a liquid. The pH test has a wide range of uses in medicine, chemistry, and agriculture. Under standard conditions the pH number indicates when the liquid is acidic ($\text{pH} < 7$), neutral ($\text{pH} = 7$) or alkaline ($\text{pH} > 7$) with a range between 0 and 14 (figure 39) [11].

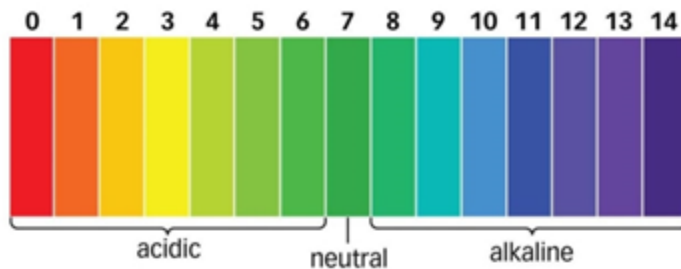


Figure 39: pH Scale [11]

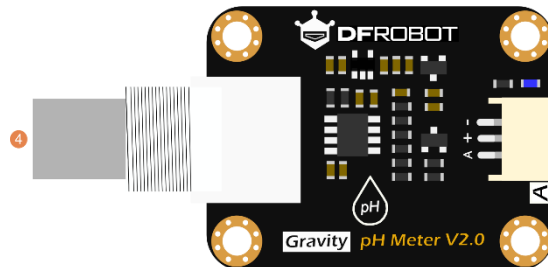


Figure 40: Board Pin mapping [12]

The pin mapping of the pH sensor is shown on Figure 40. The sensor uses one signal wire to transmit data to the microcontroller (pin 3) and is connected to an analog input. Power comes from separate a pin 3.3 up to 5.5V (pin 2) and ground wires (pin 1). At pin 4 the pH probe connector is connected.

2.10.5 Air Quality Sensor - MQ-135

MQ-135 is an air quality sensor that is suitable for detecting gases like Ammonia (NH_3), Sulfur (S), Benzene (C_6H_6), CO_2 and other harmful gases. When the level of these gases surpasses a threshold limit in the air, the analogue output pin, outputs an analogue voltage which can be used to extract the level of these gases in the atmosphere [13]. The MQ-135 operates from 2.5V up to 5.0V and it consumes about 150mA. The sensor provides both digital and analogue output.



Figure 41: MQ-135 Pin mapping [13]

The pins of the MQ-135 air quality sensor can be seen in figure 41. Pins one and three are connected to the ground of the microcontroller, whereas pin 2 is connected to the voltage supply of 5V, and finally pin four is connected to an analog pin of the microcontroller where it extracts the raw data of the sensor. In order for the MQ-135 sensor to extract the correct values, it needs to power up for a pre-heat duration. This pre-heat time is normally between 30 seconds to a couple of minutes.

2.10.6 Light Intensity Sensor – Custom made Using GL5516 LDR

For the purposes of this project the GL5516 LDR (Light Dependant Resistor) sensor was used. The GL5516 LDR sensor is a light dependant resistor which is constructed from a semiconductor materials and the conductivity changes based on the intensity of the light, called photoconductivity. A LDR sensor can be used in light-sensitive detector circuits and light and dark activated switching circuits. The sensor's size is 5mm x 2mm and is functioning with 5V [14].

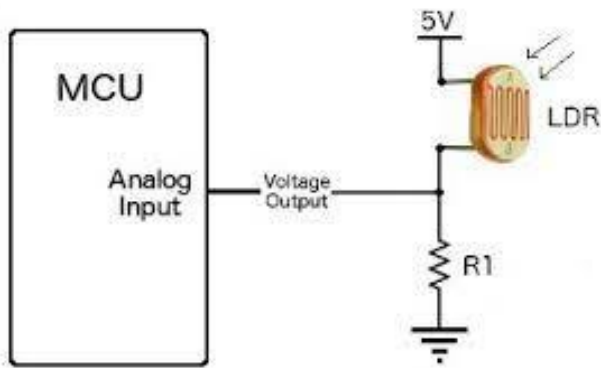


Figure 42: LDR in voltage divider configuration

The GL5516 LDR sensor is connected to the microcontroller in voltage divider configuration, as shown on figure 42. The voltage that appears at the analogue input (A1) will vary depending on the amount of light intensity that is hitting the

sensor. The LDR is connected to 5V. A pull-down resistor is required for the wiring of the sensor. A 10 k Ω resistor (R1) was chosen for the purposes of this project [15].

2.10.7 Soil Moisture Sensor – Custom made

Soil moisture sensors estimate volumetric water content in the soil. Most of them are stationary and are placed in predetermined locations and depths in the field. By using some other property of the soil, such as electrical resistance, dielectric constant, or interaction with neutrons, as a proxy for the moisture content the sensor measures the soil moisture in the field. In this project the estimation of the soil moisture is done by the measurement of the electrical resistance of the soil [16].

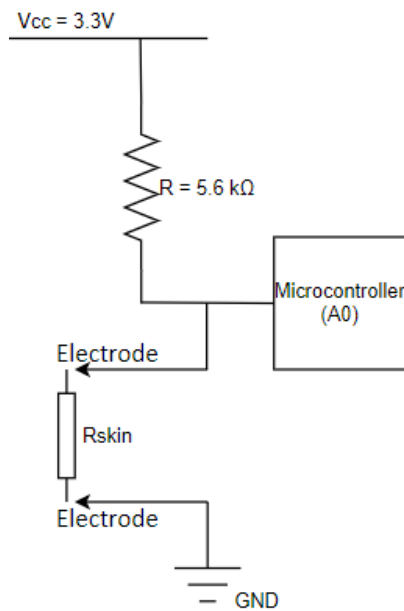


Figure 43: Soil Moisture Circuit

To calculate the resistance of the soil, a standard voltage divider circuit with two electrodes was implemented (figure 26). The circuit is operating with 3.3V and it is connected to an analogue input of the microcontroller (A4). The soil moisture circuit uses a 5.6 k Ω resistor which was selected after a big amount of experimentation. Also two electrodes are plugged in the soil in order to measure the electrical resistance of the soil (Figure 43).

2.10.8 References

- [1] T. Goldammer, "Greenhouse Managements - A Guide to Operations and Technology", Apex Publishers, ISBN (13): 978-0-9675212-4-4, 2021.
- [2] Light Science Technologies, "The importance of sensors and data for the smart greenhouse", Online Posting: <https://lightsciencetech.com/sensors-data-smart-greenhouses/> [Accessed 1/6/23].

- [3] O. Räsänen, "Seven Different Greenhouse Sensors Explained", April 21, 2022, Online Posting: <https://ruuvi.com/seven-different-greenhouse-sensors-explained/> [Accessed 1/6/23].
- [4] Renke, "8 Types Of Sensors For Best Greenhouse Remote Monitoring Systems", July 26, 2021, Online Posting: <https://www.renkeer.com/sensors-for-greenhouse-remote-monitoring-systems/> [Accessed 1/6/23].
- [5] STMicroelectronics, "STM32 Nucleo-64 development board with STM32F303RE MCU, supports Arduino and ST morpho connectivity," 2022. [Online]. Available: <https://www.st.com/en/evaluation-tools/nucleo-f303re.html> [Accessed 11 4 2022].
- [6] R. Elektronische, "uLCD-144-G2," 2021. [Online]. Available: <https://www.rutronik24.com/product/4d+systems/ulcd-144-g2/12405391.html> [Accessed 11 4 2022].
- [7] adafruit, "DHT11 basic temperature-humidity sensor," 2020. [Online]. Available: <https://www.adafruit.com/product/386#description> [Accessed 11 4 2022].
- [8] Components101, "DHT11-Temperature and Humidity Sensor," 2021. [Online]. Available: <https://components101.com/sensors/dht11-temperature-sensor> [Accessed 11 4 2022].
- [9] S. Campbell, "HOW TO SET UP THE DHT11 HUMIDITY SENSOR ON AN ARDUINO," 2015. [Online]. Available: <https://www.circuitbasics.com/how-to-set-up-the-dht11-humidity-sensor-on-an-arduino/> [Accessed 11 11 2022].
- [10] C. E. Media, "NTC Thermistor," 2021. [Online]. Available: <https://eepower.com/resistor-guide/resistor-types/ntc-thermistor/> [Accessed 11 4 2022].
- [11] J. Consulting, "What is pH?," 2020. [Online]. Available: <https://www.jansanconsulting.com/ph-scale.html> [Accessed 13 4 2022].
- [12] DFROBOT, "SKU:SEN0161-V2," 2018. [Online]. Available: https://wiki.dfrobot.com/Gravity_Analog_pH_Sensor_Meter_Kit_V2_SKU_SEN0161-V2 [Accessed 13 4 2022].
- [13] Q. components, "MQ-135 Air Quality Gas Sensor Module," 2022. [Online]. Available: <https://quartzcomponents.com/products/mq-135-air-quality-gas-sensor-module> [Accessed 14 4 2022].
- [14] H. digital, "GL5516 Light Dependent Resistor LDR 5MM," 2022. [Online]. Available: <https://www.hellasdigital.gr/electronics/sensors/light-and-color-sensors/gl5516-light-dependent-resistor-ldr-5mm/> [Accessed 15 4 2022].

- [15] Cactus.io, "How to Hookup Light Dependent PhotoResistor (LDR) to an Arduino," 2019. [Online]. Available: <http://cactus.io/hookups/sensors/light/ldr/hookup-arduino-to-ldr-sensor> [Accessed 15 4 2022].
- [16] "Anonymous," 2021. [Online]. Available: https://en.wikipedia.org/wiki/Soil_moisture_sensor [Accessed 17 4 2022].

2.11 Vegetation Indexes

Multispectral imaging captures multiple image layers with different wavelength bands. A multispectral image typically consists of four bands with RGB (Red, Blue, and Green) and Near Infrared with a wavelength range of 750 – 900 nm.

The analysis of multispectral imaging through geographic information system software, such as the '*Free and Open Source*' QGIS may produce various vegetation indexes and maps to support precision agriculture. QGIS is a software in which geospatial information can be edited, analysed and visualised and it can be utilized in remote sensing. Raster calculator (stock tool) is used to load raster band layers perform mathematical operations on raster data, on the basis of existing raster pixel values [1]. Raster data refers to pixelated data (matrix of pixels) where every pixel corresponds to a certain geographical location and each raster contains spatial information (continuous or categorical) about that location.

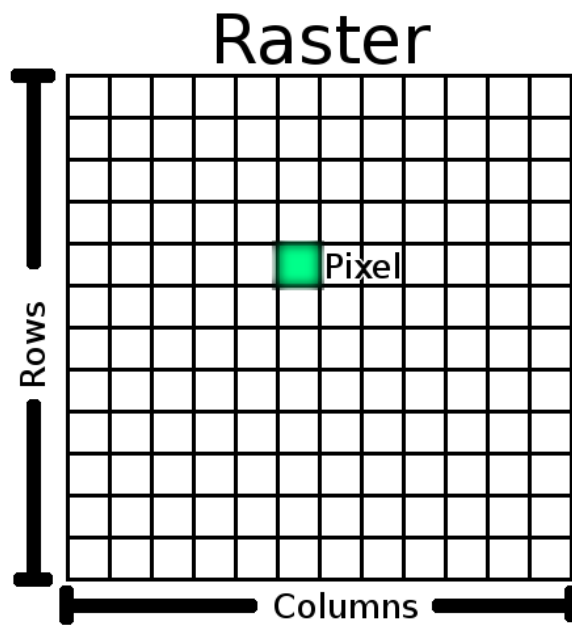


Figure 44 A raster dataset is composed of a matrix of pixels representing a geographical region, with each pixel connected to certain spatial information of that region [1]

Example data from multispectral camera is presented by Figures 45 to 49. The 4 band data is divided in Red, Green, NIR and Red Edge. It is evident that to the human eye there are minor differences between the data. However, as it is evident in the following analysis each index provides different valuable information,

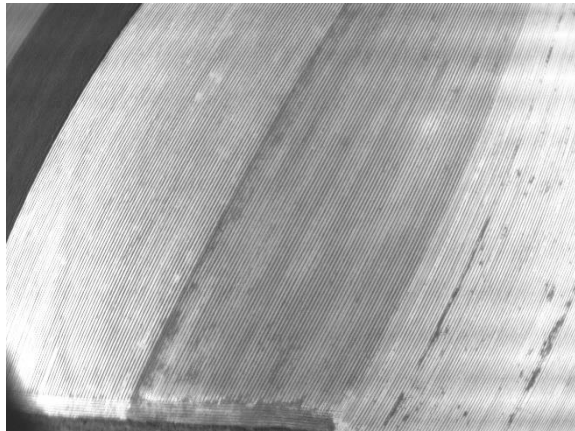


Figure 45 Green



Figure 46 NIR

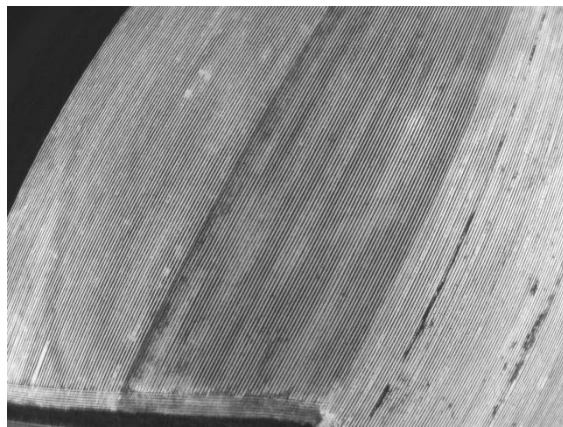


Figure 47 RED

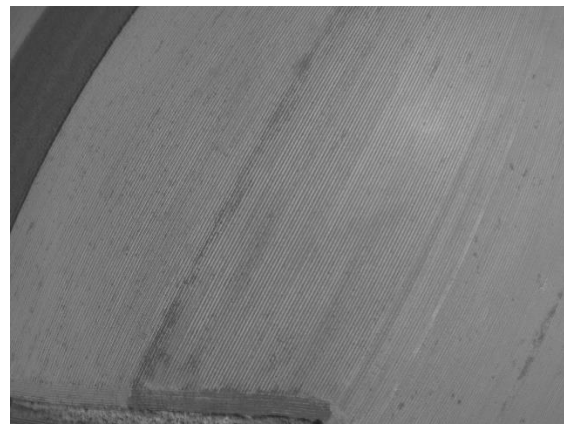


Figure 48 REDGE

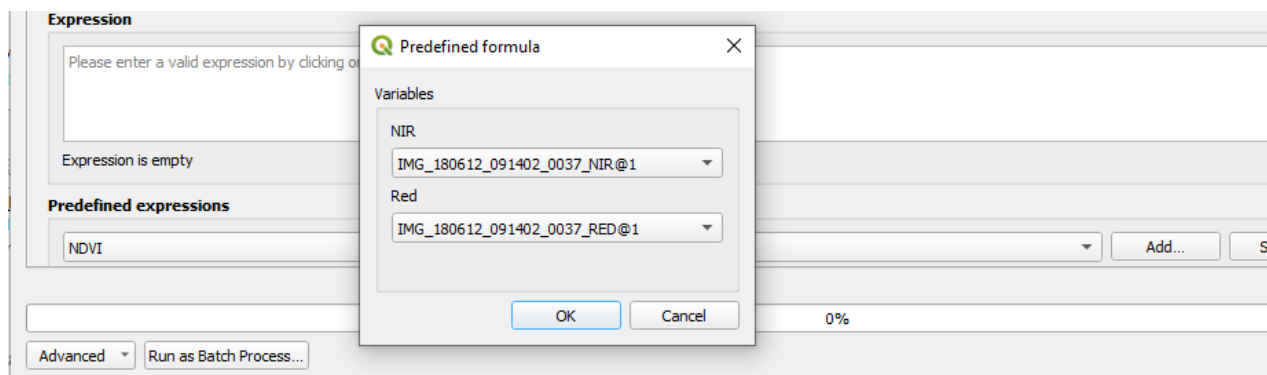


Figure 49 Calculation of NDVI with raster calculator in QGIS

2.11.1 NDVI (Normalized Difference Vegetation Index)

NDVI is one of the most popular indexes used for vegetation assessment. Research suggests that the NDVI is effective for the classification of different vegetation between savannah, dense forest, non-forest, and agricultural fields and identifies seasonal differences [1]. Since healthy vegetation with more chlorophyll content absorbs light within the blue and red wavelengths spectrum and reflects near Infrared (NIR) and green wavelengths the index may be calculated using the Red and Near Infrared channels, with equation (1).

$$\text{NDVI} = \frac{\text{NIR}-\text{Red}}{\text{NIR}+\text{Red}} \quad (1)$$

The result of the calculation provides a value between -1 and +1. High reflectance in the Near Infrared band and low reflectance in the red channel will generate a higher NDVI value. NDVI index from 0.6 – 0.9 is related to dense vegetation similar to tropical forests or crops at the growth peak [2] [3].

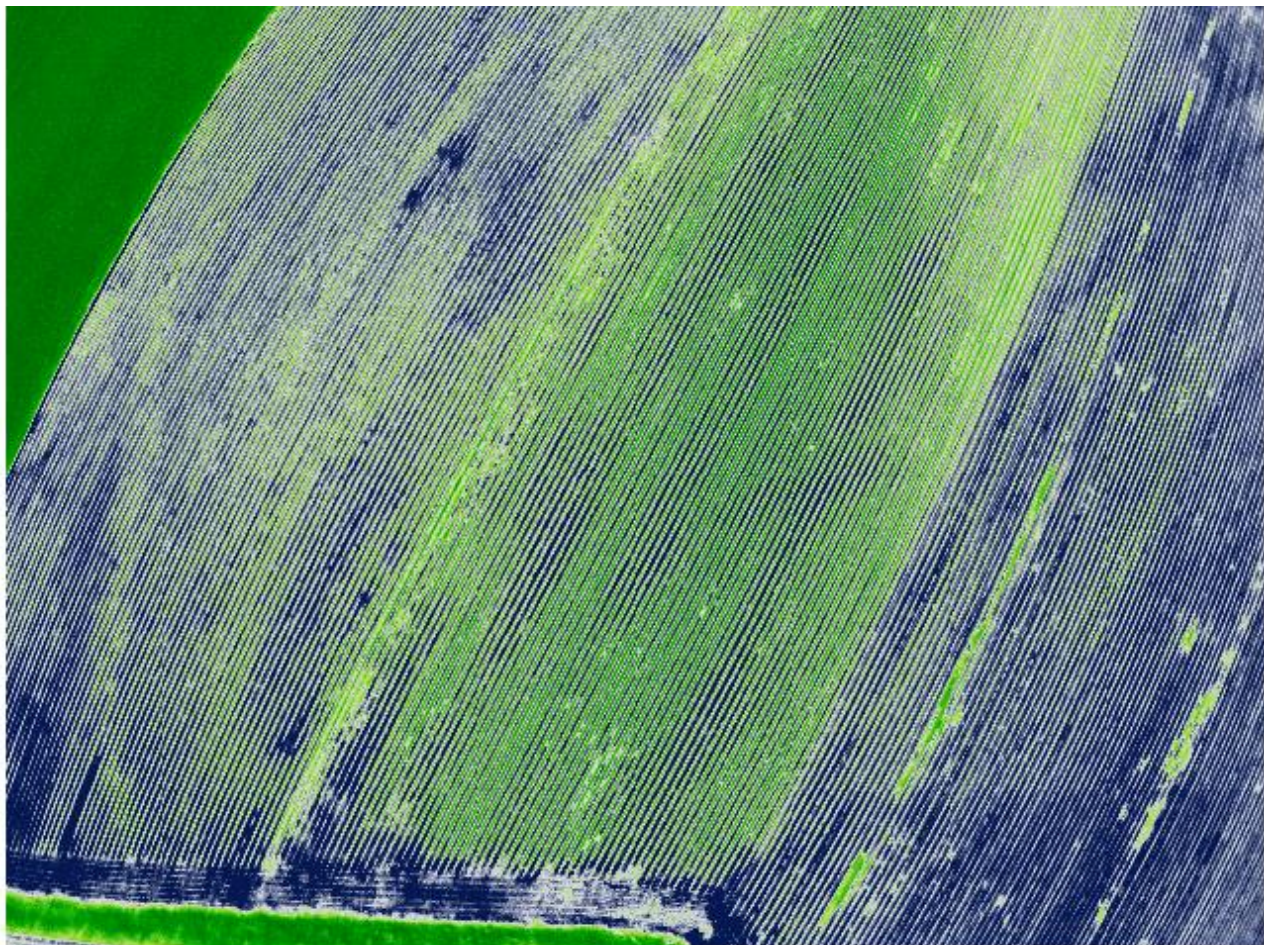


Figure 50 NDVI result of analysis

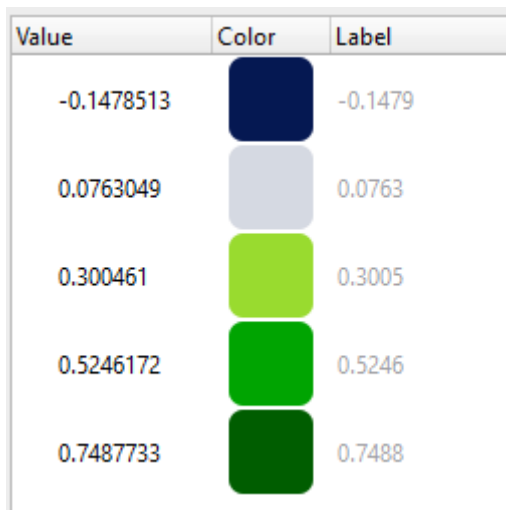


Figure 51 Colour Ramp with corresponding NDVI values

The histogram in 52 illustrates a histogram produced in QGIS, which presents the distribution of pixel values in the analysed NDVI image. As may be observed the frequency of negative values is greater which implies that the surface with no vegetation such as bare soil, rocks or water bodies is larger. Healthy vegetation with an NDVI value of approximately 0.6 is also present in the analysed image but significantly smaller.

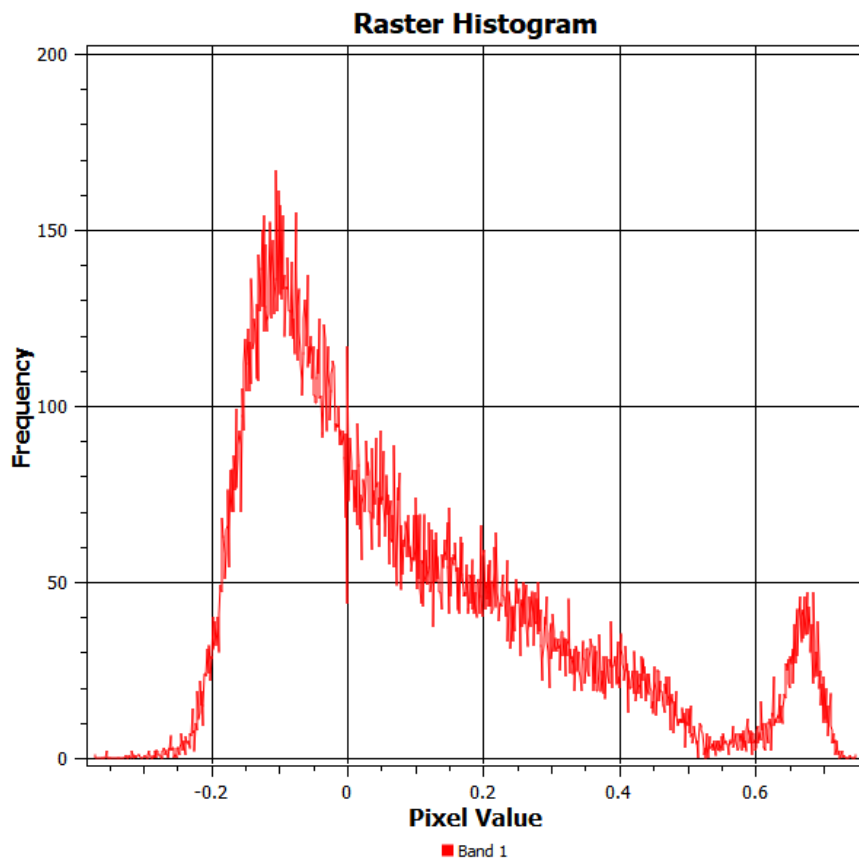


Figure 52 Histogram on NDVI

2.11.2 (NDWI) Normalized Difference Water Index

The (NDWI) Normalized Difference Water Index was also produced using QGIS. This index can be calculated using equation 2.

$$NDWI = (GREEN - NIR) / (GREEN + NIR) \quad (2)$$

NDWI provides information about the likelihood of water body presence. In this case, the generated value is also within -1 and +1 range where NDWI values closer to 1 generally suggest the presence of water

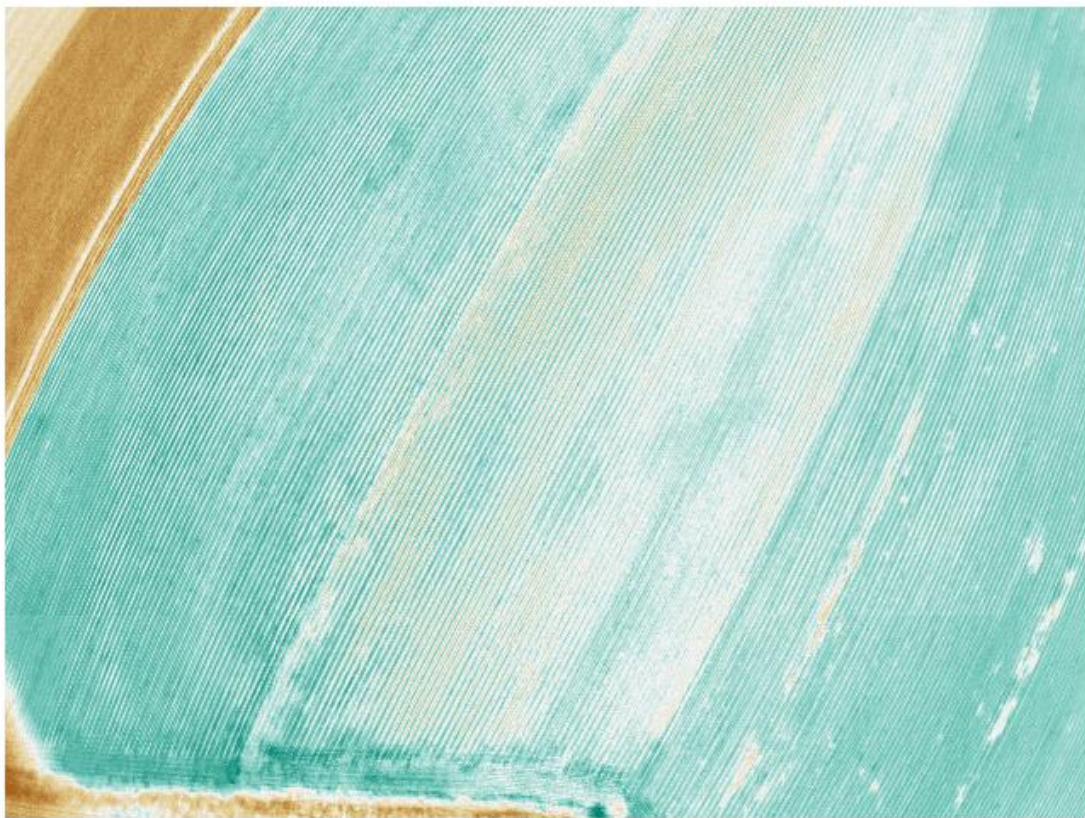


Figure 53 NDWI calculated with QGIS

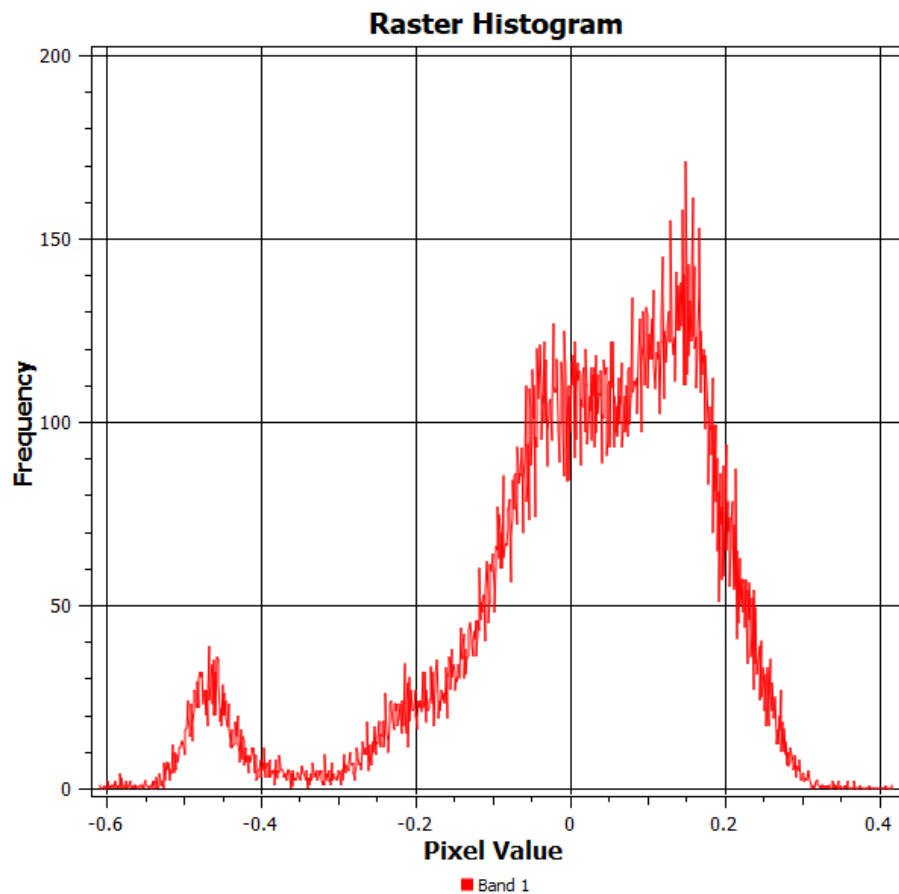


Figure 54 Histogram for NDWI

Figure 53 presents the NDWI calculated with QGIS whereas the histogram in Figure 54 illustrates the corresponding histogram where the largest NDWI value is approximately 0.42. However, it is important to note that there is no universal threshold value that could be considered in any given analysis [4]. Therefore a study of the area must be performed to determine the threshold value since various parameters such as atmospheric conditions and other landscape characteristics may yield different results.

2.11.3 OSAVI (*Optimized Soil-Adjusted Vegetation Index*)

OSAVI is another vegetation index which is based on soil adjusted vegetation index (SAVI) but uses a constant value of 0.16 to decrease the soil background influence [5]. According to studies, this value provides a more optimized calculation of vegetation cover by adjusting the sensitivity to soil brightness which may undermine the reliability of the NDVI. It is found to be more effective in areas with sparse vegetation where there is visible soil. Equation 3 is the formula for calculating the OSAVI [6].

$$\text{OSAVI} = \frac{\text{NIR} - \text{R}}{\text{NIR} + \text{R} + 0.16} \quad (3)$$

2.11.4 NDRE (*Normalized Difference Red Edge Index*)

NDRE is an index used to evaluate the health of crops by estimating the amount of chlorophyll content in the plants. In contrast with the NDVI, the formula for calculating NDRE uses REDGE band (with a wavelength of 717 nm) instead of the red band (equation 4). Research suggests that NDRE may be more suitable for the evaluation of leaves since they have better absorption in REDGE wavelength than red [7]. The NDVI can only evaluate the health status of vegetation with the red-visual band which is absorbed only on the top of the canopy, but it cannot contribute to the evaluation of the lower levels of the plants when there are layers of leaves [8]. The selection of NDRE might be preferable between the middle and late growth stages when the leaves of the crop have a denser concentration of chlorophyll and the REDGE wavelength will be more absorbed than the red wavelength. However, it may not be as effective as NDVI for the evaluation of larger land areas [7].

$$\text{NDRE} = \frac{\text{NIR} - \text{REDGE}}{\text{NIR} + \text{REDGE}} \quad (4)$$

2.11.5 GNDVI (Green Normalized Difference Vegetation Index)

This index utilizes the green channel of the multispectral image. It can serve as an indicator of photosynthetic activity within the vegetation cover and identify variation and levels of greenness in the crop [9]. GNDVI is also more effective in estimating nitrogen and moisture content in the crop canopy [10]. GNDVI is used in evaluating mature vegetation.

$$GNDVI = \frac{NIR - GREEN}{NIR + GREEN} \quad (5)$$

2.11.6 LCI (Leaf chlorophyll index)

This index is used to calculate the amount of chlorophyll in the leaves and is more reliable in the late summer months since the patterns are correlated with the crops' final yield [11].

$$LCI = \frac{NIR - REDGE}{NIR + RED} \quad (6)$$

2.11.7 References

- [1] S. Huang, L. Tang, J. P. Hupy, Y. Wang and G. Shao, "A commentary review on the use of normalized difference vegetation index (NDVI) in the era of popular remote sensing," *Journal of Forestry Research*, vol. 32, no. 1, pp. 1-6, 2021.
- [2] Remote Sensing Phenology , "NDVI, the Foundation for Remote Sensing Phenology," USGS, 27 November 2018. [Online]. Available: [https://www.usgs.gov/special-topics/remote-sensing-phenology/science/ndvi-foundation-remote-sensing-phenology#:~:text=High%20NDVI%20values%20\(approximately%200.6,at%20their%20peak%20growth%20stage..](https://www.usgs.gov/special-topics/remote-sensing-phenology/science/ndvi-foundation-remote-sensing-phenology#:~:text=High%20NDVI%20values%20(approximately%200.6,at%20their%20peak%20growth%20stage..) [Accessed 3 February 2024].
- [3] GISGeography, "What is NDVI (Normalized Difference Vegetation Index)?," GISGeography, 14 October 2023. [Online]. Available: <https://gisgeography.com/ndvi-normalized-difference-vegetation-index/>. [Accessed 3 February 2024].
- [4] Z. Fang-fang, Z. Bing, L. Jun-sheng, S. Qian, W. Yuan feng and S. Yang, "Comparative Analysis of Automatic Water Identification," *Procedia Environmental Sciences*, vol. 11, pp. 1482-1487, 2011.

- [5] A. Vasudevan, A. D. Kumar and N. S. Bhuvaneswari, "Precision farming using unmanned aerial and ground vehicles," 2016 IEEE technological innovations in ICT for agriculture and rural development (TIAR), pp. 146-150, 2016.
- [6] R. R. Ferna, E. A. Foxley, A. Bruno and M. L. Morrison, "Suitability of NDVI and OSAVI as estimators of green biomass and coverage," Ecological Indicators, vol. 94, pp. 16-21, 2018.
- [7] B. Boiarskii and H. Hasegawa, "Comparison of NDVI and NDRE Indices to Detect Differences," International Conference on Applied Science, Technology and Engineering, no. 4, pp. 20-29, 2019.
- [8] L. Osborn, "NDVI vs. NDRE: What's the Difference?," Sentera, 4 February 2022. [Online]. Available: <https://sentera.com/resources/articles/ndvi-vs-ndre-whats-the-difference/> . [Accessed 4 2 2024].
- [9] A. A. Gitelson, Y. J. Kaufman and M. N. Merzlyak, "Use of a green channel in remote sensing of global vegetation from EOS-MODIS," Remote Sensing of Environment, vol. 58, no. 3, pp. 289-298, 1996.
- [10] M. V. Gordillo-Salinas, H. F. Magdaleno, C. A. Ortiz-Solorio and A. R. Ramírez, "Evaluation of nitrogen status in a wheat crop using unmanned aerial vehicle images," Chilean journal of agricultural research, vol. 81, no. 3, 2021.

2.12 Commercially Available mmWave Radar Sensors

The current market availability of mmWave radar sensors has steered this investigation in mainly two directions: one using 2-DoF (Degrees of Freedom) sensors that support ranging and azimuth measurements and one using 3-DoF sensors that additionally measure the elevation of targets. For each of these cases we performed a precision analysis of the most predominantly-used mmWave ranging sensors currently in the market and thereafter used the ranging/angular information to conduct positioning using various methods. For the 2DOF case we consider sensors that have the ability to measure range and azimuth (the Texas Instruments IWR1642Boost and the Infineon Distance2Go) while for the 3DOF that additionally measures elevation we used the Texas Instruments IWR1843.

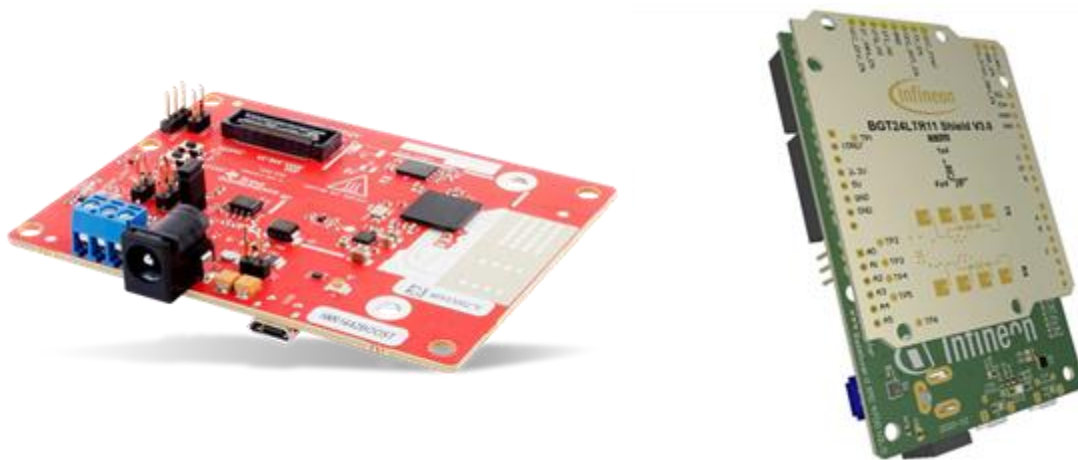


Figure 55: 2-DOF mmWave Sensors: TI's IWR1642BOOST (left) and Infineon's Distance2Go (right)

The two mmWave radar sensors that were used for the 2-DOF precision analysis were the Texas Instruments (TI) IWR1642BOOST and Infineon Distance2Go. The TI sensor is equipped with 4 receiving (Rx) and 2 transmitting (Tx) antennas operating at frequencies between 76-81GHz with a 120-degree field of view and ranging capabilities of up to 72 meters. In contrast, the Infineon Distance2Go mmWave sensor is equipped with 1 Rx and 1 Tx antenna and operates between 24-26GHz with a field of view of 20 degrees and a maximum detection range of around 20 meters. While the TI sensor performs range and angle measurements, the Infineon one can only measure range. The experimental setup involved utilizing a DJI Air 2S drone as the target for ranging and angular measurements. It is a compact drone with dimensions of 183.0X77.0X253.0mm.

Similarly to IWR1642BOOST, the IWR1843BOOST possesses a Frequency Modulated Continuous Wave (FMCW) transceiver which enables the measurement of range, azimuth angle and velocity of the target. However, due to an additional TX antenna, in addition to the azimuth angling information, it is also able to provide the elevation data of the target. A similar system setup was used for this sensor like the one used for the IWR1642BOOST in which each sensor

is connected to a Raspberry PI, through which the collected context is parsed and then sent to a central PC through a UDP connection.

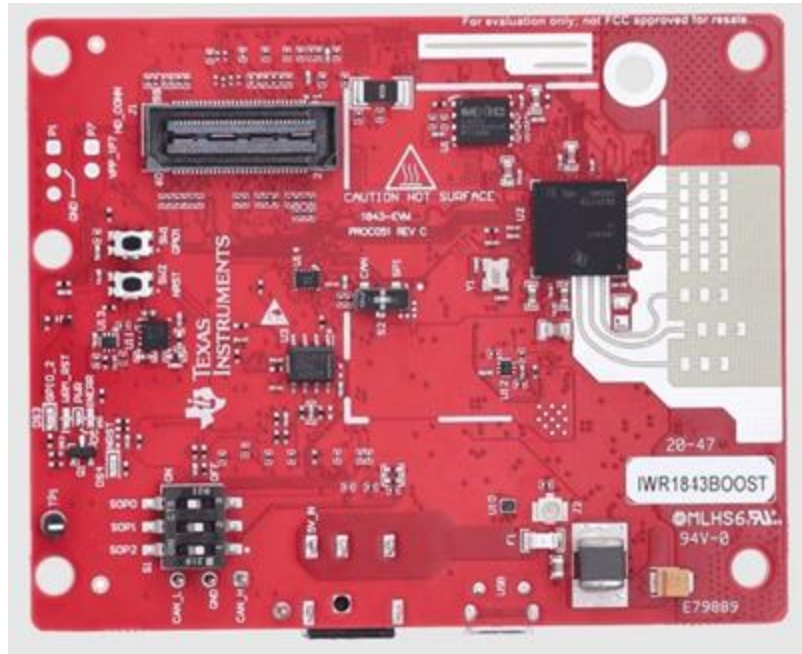


Figure 56: IWR1843BOOST Sensor

For the indoor positioning purposes of the DEMETRA project 5 such sensors will be used.

3 Used Cases and Scenarios

A few measurement and simulation scenarios have been defined for the operational requirements and technical objectives of the project described in section **Error! Reference source not found.** to be met.

Measurement scenarios include 3 types of environments (indoor cluttered, indoor open-space, outdoor open space) and different mobility use cases for each. For all the environments Static measurements are going to be conducted in order to access the angle and ranging precision at different orientations and distances respectively and will be used to test the accuracy of the geometric 3D positioning models. It is worth noting that the output of the precision analysis (ranging error) will form the input to the Kalman filters which will be used in the mobility use-cases.

The mobility use-cases are intended to be implemented to demonstrate accuracy of the 3D positioning system when context from mmWave sensors is fused with context from IMU with use of various types of Kalman Filters. For the indoor cases, only low mobility will be considered which involves the target (preferably drone, but also balls and humans will be considered) moving at low pedestrian-level speeds typically between 0.6-1.4m/s. For the outdoor case we will also consider a use case of high mobility with the speed of the target set up to 20m/s (depending on the drone capability). For all the only one target will be used in the environment and visual AI will be optionally used if time allows it.

Simulation scenarios will be used also to assess the sensitivity of the implemented methods under various uncertainties. They will form an easy way to generate much location-specific data (ranges, angles) and introduce to it different levels of uncertainties/inaccuracies according to the precision analysis that will be conducted in the static use cases.

3.1.1 Indoor Cluttered Environment

	Static Case	Low Mobility
Environment	Indoor	
Environment Dimensions (72pprox..)	50-60 m ²	
Clutter	HIGH – Consisting of benches, equipment on the benches, many metallic surfaces spread around the room	
Clutter Mobility	Stationary	Stationary
Number of Sensors	Up to 5	
Target Mobility	Stationary	Pedestrian-Level (0.6-1.4m/s)
Number of Targets	1	1
Kalman Filtering	No	Yes
Targets	Drones and/or Balls and/or Humans	
3D Positioning	Yes	

Sensors	mmWave, Cameras	mmWave, IMU, Cameras
Applicability/Investigations	For precision analysis and preliminary 3D positioning using geometric methods without fusing it with data from IMUs	For 3D positioning using data from both mmWave and IMUs
Parameters to Measure	<ul style="list-style-type: none"> • Distance from Sensors • AoD from Sensors. (mostly azimuth but also elevation if the sensors support it) 	<ul style="list-style-type: none"> • Distance from Sensors • AoD from Sensors. (mostly azimuth but also elevation if the sensors support it) • IMU Data (Accelerometer [x,y,z], gyroscope [x,y,z] and magnetometer [x,y,z])

3.1.2 Indoor Open space Environment

	Static Case	Low Mobility
Environment	Indoor	
Environment Dimensions (approx.)	50-60 m ²	
Clutter	Low – Consisting of desks and chairs. No metallic surfaces	
Clutter Mobility	Stationary	Stationary
Number of Sensors	Up to 5	
Target Mobility	Stationary	Pedestrian-Level (0.6-1.4m/s)
Number of Targets	1	1
Kalman Filtering	No	Yes
Targets	Drones and/or Balls and/or Humans	
3D Positioning	Yes	
Sensors	mmWave, Cameras	mmWave, IMU, Cameras
Applicability/Investigations	For precision analysis and preliminary 3D positioning using geometric methods without fusing it with data from IMUs	For 3D positioning using data from both mmWave and IMUs
Parameters to Measure	<ul style="list-style-type: none"> • Distance from Sensors • AoD from Sensors. (mostly azimuth but also elevation if the sensors support it) 	<ul style="list-style-type: none"> • Distance from Sensors • AoD from Sensors. (mostly azimuth but also elevation if the sensors support it) • IMU Data (Accelerometer [x,y,z], gyroscope [x,y,z] and magnetometer [x,y,z])

3.1.3 Outdoor Open Space Environment

	Static Case	Low Mobility	High Mobility
Environment	Outdoor		
Environment Dimensions (approx.)	50-100 m ² Depending on the capability of the sensors		
Clutter	None – Open Space		
Clutter Mobility	Stationary		
Number of Sensors	Up to 5		
Target Mobility	Stationary	Pedestrian-Level (0.6-1.4m/s)	Average Drone Mobility (up to 20m/s)
Number of Targets	1	1	1
Kalman Filtering	No	Yes	Yes
Targets	Drones and/or Balls and/or Humans		
3D Positioning	Yes		
Sensors	mmWave, Cameras		
Applicability/Investigations	For precision analysis and preliminary 3D positioning using geometric methods without fusing it with data from IMUs		For 3D positioning using data from both mmWave and IMUs
Parameters to Measure	<ul style="list-style-type: none"> • Distance from Sensors • AoD from Sensors. (mostly azimuth but also elevation if the sensors support it) • IMU Data (Accelerometer [x,y,z], gyroscope [x,y,z] and magnetometer [x,y,z]) 		

4 Metrics/Key Performance Indicators and Targets

To assess the performance of the mmWave Sensors and thereafter the accuracy of the developed 3D positioning algorithms the following metrics/KPIs have been set together with their target values. The target values have been selected based on what is currently reported in the literature but also in conjunction with the maximum dimension of the target to be detected.

4.1 Precision Analysis KPIs

For the precision analysis the actual error between the true value and the measured value will be recorded for both the ranging measurement and the angle measurements. This means that this error can either be positive or negative. For every measurement i the error can be calculated as follows

$$\text{Error}_i = \text{True Value}_i - \text{Measured Value}_i$$

To estimate the average error of the measurement, only positive values will be considered. In this respect we will calculate two metrics. These are the average absolute error and the mean squared error calculated using the following equations for m measurements

$$\text{Average Absolute Error} = \frac{1}{m} \sum_{i=1}^m |\text{Error}_i|$$

$$\text{RMS Error} = \sqrt{\frac{1}{m} \sum_{i=1}^m \text{Error}_i^2}$$

4.2 3D Positioning Analysis KPIs

For the 3D positioning analysis, the most important performance parameter is distance error from the true value. This is the Euclidean distance between the ground truth 3D points and the one estimated by the positioning algorithm.

Given that:

$$\text{True Location (Ground truth)} = [x_T \quad y_T \quad z_T]$$

$$\text{Estimated Location} = [x_P \quad y_P \quad z_P]$$

The distance error for a single estimation is estimated as follows:

$$3D \text{ Error}_i = \sqrt{(x_T - x_P)^2 + (y_T - y_P)^2 + (z_T - z_P)^2}$$

The average absolute error and RMS error can be estimated using the two equations above.

As it is also important to access the error in each axis the following errors need to be estimated

$$\Delta x_i = x_{Ti} - x_{Pi}$$

$$\Delta y_i = y_i - y_{Pi}$$

$$\Delta z_i = z_{Ti} - z_{Pi}$$

Likewise the average absolute error and RMS error can be estimated using the two equations above.

5 Technical Specifications

Considering the technical objectives, operational requirements, use cases and scenarios described above the following equipment is needed:

5.1 Hardware

Type	Model Options	Quantity
mmWave Sensors	Texas Instruments IWR1642BOOST	5
	Texas Instruments IWR1843BOOST	
	Infineon DISTANCE2GOL	
Drone	DJI Air 2S, DJI Mavic 3M	1
	Any other custom-built drone	
IMU	9DOF IMU - 9250	2
Cameras	Open CV AI Camera OAK-D	2
Microcontrollers	Raspberry Pi4	5
	ESP32 with Wifi Connection	2
Laptop Computer	Any Windows Based Computer	1
Desktop Computer	Any Windows Based Computer	1
USB-3 to USB-c cables	At least 5 meters to	5
Power Banks to power the microcontrollers	USB output	8
UPS for the central desktop PC	Any	1

5.2 Software

The following software tools will be needed:

- MATLAB
- Python
- Arduino IDE

- PyCharm or Visual Studio Code
- SQL Server Express
- YOLO Convolutional Neural Network Algorithm
- DJI Terra
- Open Source QGIS
- GPS-SDR-SIM: <https://github.com/osqzss/gps-sdr-sim> (needs to be compiled in visual studio to run)
- Visual studio: <https://visualstudio.microsoft.com/vs/community/>
- Mission Planner: <https://ardupilot.org/planner/docs/mission-planner-installation.html>
- PothosSDR: <http://downloads.myriadrf.org/builds/PothosSDR/>
- SatGen V3: <https://www.labsat.co.uk/index.php/en/customer-area/software-firmware>
- Latest RINEX navigation ephemerides broadcast brdc file from Nasa. An account is required which can be created free: <https://cddis.nasa.gov/archive/gnss/data/daily/2023/brdc/>

6 Summary of all Proposed KPIs

6.1 Greenhouse Mentoring System

The greenhouse monitoring system should have the following characteristics:

- Temperature with accuracy of $\pm 2^{\circ}\text{C}$
- Relative Humidity with accuracy $\pm 10\%$
- Measurement and identification of CO₂ gas
- Measurement of pH with accuracy $\pm 10\%$
- Development of a Light Intensity Sensor
- Development of a custom made Soil Moisture sensor with accuracy $\pm 10\%$

6.2 Image Processing

Development of image processing capability for small UAV applications (compact, lightweight and low power).

- Achieve state of the art or higher FPS with an accuracy higher than 80%.
- Reduce power consumption on the single board computer
- Dataset for insects in Cyprus
- Detection at distance of maximum 6 meters

6.3 UAV Flight and Multispectral Data Collection

- Flight stability and immunity from vibrations
- Multispectral Data Collection

6.4 Multispectral Image Processing

- Successful multispectral data analysis for various indices using software DJI Terra and open source QGIS

6.5 Indoor Positioning

Using AI Cameras or mmWave Radar sensors

- Sub-meter accuracy

6.6 Indoor Positioning by GPS Conversion and Retransmission

- Sub-meter accuracy